communications biology

A Nature Portfolio journal

Article

https://doi.org/10.1038/s42003-025-07857-8

Comprehensive co-expression network reveals the fine-tuning of *AsHSFA2c* in balancing drought tolerance and growth in oat

Ningkun Liu[1,2,4], Wei Li[1,2,4], Yujie Qin[1,4], Yange Yun[1], Jinjiang Yan[1], Qingbin Sun[1], Cailian Du[1], Qiang He[1,2], Shuhui Wang[1], Zhizhong Gong[1,3] & Huilong Du[1,2]

Persistent activation of drought tolerance is detrimental to plant growth and development. However, the mechanism that balances plant drought tolerance and growth remains largely undetermined. Here, we constructed a comprehensive co-expression network comprising 84 transcriptome datasets associated with growth and drought tolerance in oats. Moreover, 84 functional modules and many candidate genes related to drought tolerance and growth were identified. A key candidate gene, *AsHSFA2c* was involved in fine-tuning the balance between drought tolerance and growth by inhibiting plant growth and positively regulating drought tolerance. Then, we determined AsDOF25 as an upstream positive regulator and *AsAGO1* as the downstream target gene of *AsHSFA2c*. These results imply that the *AsDOF25-AsHSFA2c-AsAGO1* module contributes to the balance between drought tolerance and growth in oats. Our findings and resources will facilitate the identification of key genes related to drought tolerance and further studies of the genetic basis underlying strong drought tolerance in oats.

Drought, which is one of the most pressing challenges in agriculture today, often alters plant physiology, biochemistry, and molecular regulation, leading to the termination of photosynthesis and metabolic disorders, and ultimately resulting in a decrease in grain yield[1–5]. Thus, there is a critical need to identify key genes associated with the drought stress response in highly drought-resistant species or accessions and characterize their molecular regulatory mechanisms. Common oat (*Avena sativa* L., $2n = 6x = 42$, AACCDD), which is ranked seventh among cereals in terms of production (http://www.fao.org/faostat/en/; accessed May 2021), is an economically important food and feed crop cultivated worldwide and is highly adaptable to various climatic conditions, especially drought[6–8]. Therefore, identifying key genes that contribute to drought tolerance in oats has become increasingly important. However, due to the lack of a mature and stable genetic transformation system and omics data for drought stress, relatively few drought resistance-related genes have been identified in oats.

Under drought conditions, plant growth and development are seriously impaired. To cope with increasingly serious drought stress, there has been a steady increase in research on the balance between plant drought tolerance and growth[9]. There are two main viewpoints regarding the balance between plant growth and stress responses, including the allocation of limited energy and the enhanced expression of genes that promote growth to inhibit drought stress responses[9]. Research on the balance between plant drought tolerance and growth is of great significance to agricultural development. To date, many genes related to balancing drought tolerance and growth have been identified in rice, maize, wheat, and other important crops[10–12]. These studies showed that hormonal signals play a crucial role in regulating the balance between drought tolerance and growth in plants. Specifically, the interactions between abscisic acid (ABA) and indole-3-acetic acid (IAA), as well as between ABA and gibberellin (GA) are essential for maintaining the balance[12,13]. However, genes responsible for balancing drought tolerance and growth and their regulatory mechanisms remain largely unknown in oats.

In response to biotic and abiotic stresses, transcription factors play an important role in the regulation of plant growth and development. The heat shock factor (HSF) gene family is a kind of transcription factor, and is widely present in prokaryotes and eukaryotes[14]. In plants, the HSF family plays a

[1]College of Life Sciences, Institute of Life Sciences and Green Development, Hebei University, Baoding, China. [2]Hebei Basic Science Center for Biotic Interaction, Baoding, China. [3]State Key Laboratory of Plant Environmental Resilience, College of Biological Sciences, China Agricultural University, Beijing, China. [4]These authors contributed equally: Ningkun Liu, Wei Li, Yujie Qin. e-mail: huilongdu@hbu.edu.cn

central role in regulating various processes, including growth and development and responses to abiotic stresses, including heat, drought, salt, and cold stress[15–17]. Previous studies have reported that *OsHSFa7*, *OsHSFb2b*, *ZmHSF08*, *GmHSF-34*, and *TaHSFa2e-5d* played key roles in regulating drought tolerance in crops[18–22]. However, little has been reported about whether HSF family genes are involved in regulating the balance between plant drought tolerance and growth. Furthermore, the biological functions and molecular regulatory mechanisms of the HSF family in oats also remain elusive.

In this study, we constructed a comprehensive co-expression network of genes that balance drought tolerance and growth in oats. This network included 84 modules and numerous candidate genes associated with drought tolerance and growth, offering valuable resources for future analyses of drought tolerance in oats and the associated regulatory mechanisms. To verify the network's credibility, we utilized the virus-induced gene silencing (VIGS) system in oat for functional validation of several candidate modules and genes. By integrating over-expression transgenic oat lines, we characterized the function of *AsHSFA2c* in regulating the balance between drought tolerance and growth in oat. Additionally, we determined that *AsHSFA2c* was regulated by the upstream transcription factor AsDOF25 and transcriptionally repressed the downstream gene *AsAGO1*. Overall, this study provides insights into the genetic basis of drought tolerance in oats by elucidating how *AsHSFA2c* mediates the balance between drought tolerance and growth. This resource will also facilitate further investigations on the genetic basis of strong drought tolerance in oats.

Result

Co-expression network construction for oat drought response and growth

To comprehensively characterize transcriptional dynamics related to oat plant growth and drought stress response, we generated a gene expression atlas comprising 84 samples collected from cultivated oats exposed to drought stress or treated with polyethylene glycol (PEG)-6000 and hormones (ABA and IAA) (Fig. 1a, Supplemental Fig. 1a–d, and Supplemental Data 1). The correlation analysis of the 84 transcriptome samples revealed a high degree of consistency among biological replicates, all of which clustered together (Supplemental Fig. 2a). To further validate the quality of the gene expression profiles, the effects of each treatment were assessed by examining the response of marker genes (Supplemental Fig. 2b and Supplemental Data 2). Each marker gene was either up- or down-regulated after the corresponding treatment, which is consistent with previously reported patterns. For example, *AREB1* and *PP2C* were significantly induced by ABA[23,24], indicating that the treatment effectively altered the expression of these response marker genes. Gene expression analysis showed that a total of 62,242 differentially expressed genes (DEGs) were identified across all treatments (Fig. 1b, Supplemental Fig. 2c, and Supplemental Data 3). Furthermore, 13,301 DEGs were found to be shared among the drought, PEG6000, ABA, and IAA treatments, suggesting their potential role in both drought tolerance and growth in oat (Fig. 1b). As previously reported[25–29], our transcriptome data showed that a substantial number of genes exhibited opposite expression trends after IAA and drought treatments (Supplemental Fig. 2d). Meanwhile, we performed a quantitative analysis, using Fisher's exact test[30,31], to evaluate the overlap of differentially expressed genes (DEGs) between hormone treatments (ABA and IAA) and drought-related treatment (drought and PEG6000 treatments) (Supplemental Fig. 2e). The results showed that the overlapping DEGs between ABA treatment and drought-related treatment were significantly higher compared to those between IAA treatment and drought-related treatment (Supplemental Fig. 2e). Then, we conducted transcriptome analysis on genes annotated as being involved in the ABA and IAA signaling pathways. As reported previously[32,33], most of the genes explored their antagonistic patterns at the transcriptomic level (Supplemental Fig. 3a–d and Supplemental Data 4 and 5). This result further supports the reliability of our transcriptome data. Subsequently, we performed Gene Ontology (GO) and Kyoto Encyclopedia of Genes and Genomes (KEGG) analyses to functionally characterize DEGs and determine differences among treatment groups. Many of the DEGs were functionally associated with plant growth and defense responses (Supplemental Fig. 4a–b and Supplemental Data 6 and 7). For example, the DEGs responsive to the ABA treatment were mainly involved in the glutathione metabolic process, carbohydrate binding, response to water, transferase activity, and defense response. In contrast, DEGs following the IAA treatment were mainly associated with response to auxin, plant hormone signal transduction, and photosynthesis antenna proteins. For the PEG6000 treatment, DEGs were primarily involved in processes related to photosynthesis, glutathione metabolic process, response to water, phosphatidylinositol phospholipase C activity, and carbohydrate binding. In drought-treated samples, DEGs were significantly enriched in processes like glutathione metabolic process, photosynthesis, cell wall macromolecule catabolic process, and embryo development ending in seed dormancy (Supplemental Fig. 4a, b and Supplemental Data 6 and 7).

We further integrated these 84 transcriptome datasets to perform the weighted gene co-expression network analysis (WGCNA) (Fig. 1c), and combining the evidence from the correlation analysis, module classification, and functional enrichment analysis, a total of 84 functional modules were identified (Fig. 1c, d and Supplemental Data 8). Among them, the largest and smallest modules contained 6226 and 19 genes, respectively (Fig. 2a and Supplemental Data 9). To evaluate the interaction of all modules, eigengene adjacency was calculated. The heatmap showed that the modules were distinguished well from one another (Supplemental Fig. 4c). Gene functional enrichment analysis showed that many modules covered functions such as photosynthesis, plant hormone signal transduction, arginine and proline metabolism, as well as cell wall biogenesis (Fig. 1d, Supplemental Fig. 4d, and Supplemental Data 8 and 10), indicating these modules may play an important role in regulating plant growth and responding to drought stress. For example, in our network, we detected the co-expression of *PYL* (PYRABACTIN RESISTANCE 1-LIKE, oat091221), *SnRK2* (phosphatsenon-fermenting SNF1 related protein Kinase2s, oat067672) and *PP2C* (phosphatase type 2Cs, oat041125), which were the previously reported important components of a drought response-related ABA signaling pathway (Fig. 1e)[34,35], further supporting the reliability of our network. Besides, we also identified three additional genes (oat058263, oat049732, and oat079894) that were co-expressed with *PYL*, *SnRK2,* and *PP2C* (Fig. 1e). Our co-expression network may serve as a valuable resource for the oat research community, enabling the identification of functional genes or modules associated with growth and drought stress response. Additionally, it may contribute to studies on the regulation of the balance between plant drought tolerance and growth.

Candidate modules related to drought tolerance in oat

The correlation coefficients between the 84 gene modules and various treatments were evaluated, revealing that many functional modules were strongly associated with the corresponding treatments (Fig. 2a). For instance, 52 modules were closely related to drought treatment or PEG6000 treatment, indicating their potentially essential roles in regulating drought tolerance in oat (Supplemental Data 11). Among them, we randomly selected one module (Cluster 1) to show (Fig. 2b, c and Supplemental Data 12). In this module, transcription factors with connectivity greater than or equal to 5 were identified as hub transcription factors (Fig. 2c). This transcription factor network identified hub transcription factors potentially involved in oat drought stress and revealed their associated target genes. Functional enrichment analysis showed that the genes in Cluster 1 were primarily involved in the MAPK signaling pathway, flavone and flavonol biosynthesis, and calcium signaling pathways (Fig. 2b and Supplemental Data 13), which have previously been reported to be involved in drought signaling transduction[27,36,37]. Additionally, many homologous genes, such as *OsWRKY10*, *OsWRKY72*, *ANAC102*, *ANAC032*, *OsbZip25*, and *OsDREB1C*, which have been previously reported to be involved in the regulation of drought tolerance, were identified in Cluster 1 (Fig. 2c and Supplemental Data 14 and 15)[38–42]. To further validate the reliability of this drought tolerance-related module, we randomly selected five genes with

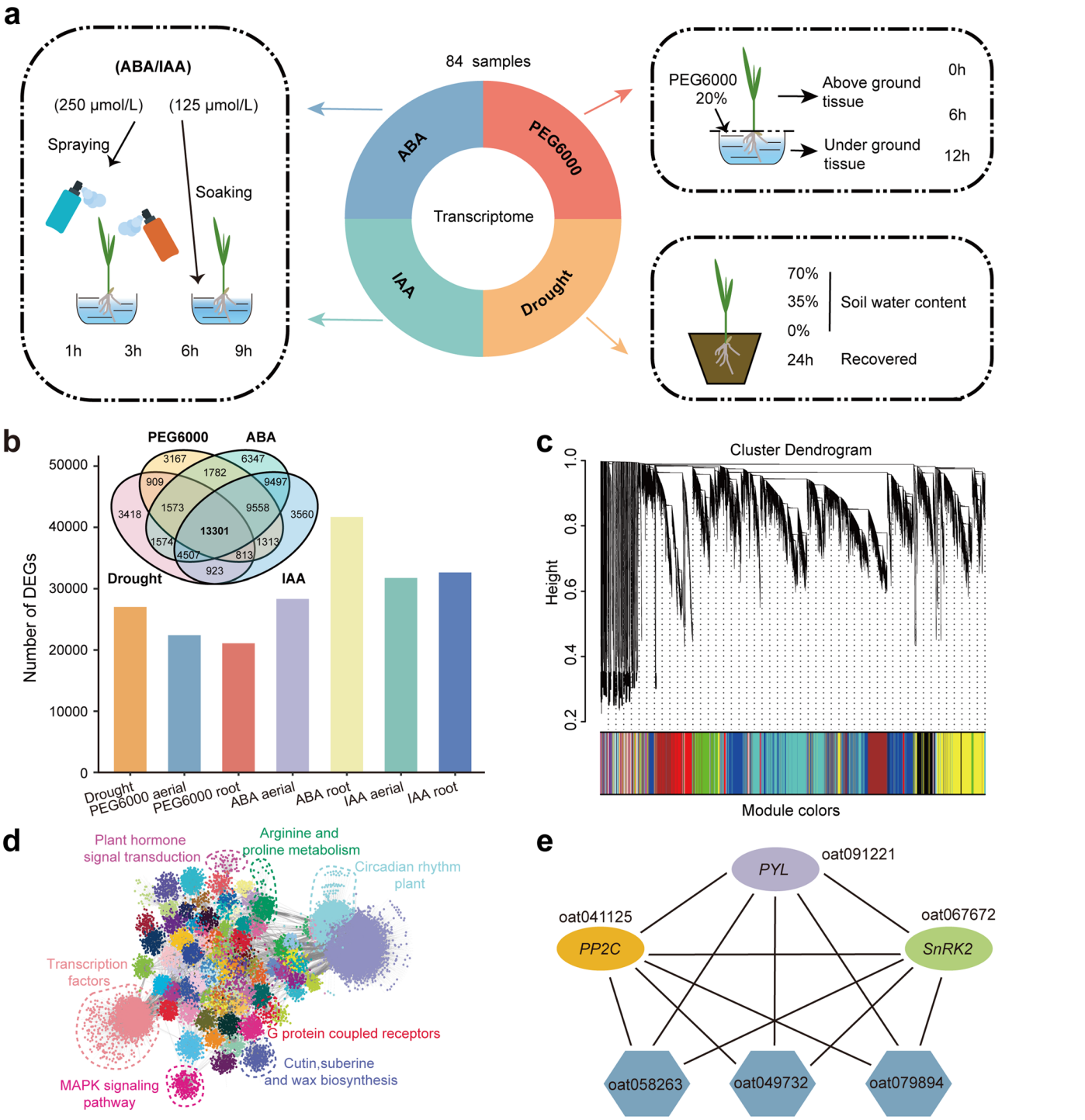

Fig. 1 | Construction of comprehensive co-expression networks that balance drought tolerance and growth in oat. a Schematic diagram of transcriptome sequencing with different treatments. **b** Identification of differential expression gene analysis. A Venn diagram presents the common and unique expressed genes in response to drought-related stress (drought and PEG6000 treatment), ABA and IAA treatments (up part), and the number of differentially expressed genes (down part). **c** Cluster dendrogram and color representation of the co-expression network modules produced by average linkage hierarchical clustering of genes based on topological overlaps. **d** Display of co-expression network modules. Based on the connectivity among modules, we demonstrated the modules in the co-expression network. Different colors represent different modules. Several modules related to drought tolerance or growth are marked along with their functions. **e** An example to prove the credibility of co-expression networks for the well-known protein-encoding genes *PYL*, *PP2C*, *SnRK2* and their correlations with other mRNAs (Gray-blue hexagon).

homologs known to be associated with drought tolerance in other species[43–47], as well as five genes with unknown function, for qRT-PCR analysis (Fig. 2d). The results showed that 9/10 genes respond to drought treatment, implying that the module was likely related to drought tolerance. To further validate the identified module, we selected the hub transcription factor *AsMYC2* (oat068987), a homolog of *TaMYC2* in wheat, as a candidate gene for functional validation. The transcription factor MYC2 has been reported to regulate drought tolerance in several plants, including *Triticum aestivum*, *Arabidopsis thaliana*, *Brassica napus*, and *Solanum lycopersicum*[48–51]. qRT-PCR assay showed that the expression of *AsMYC2*

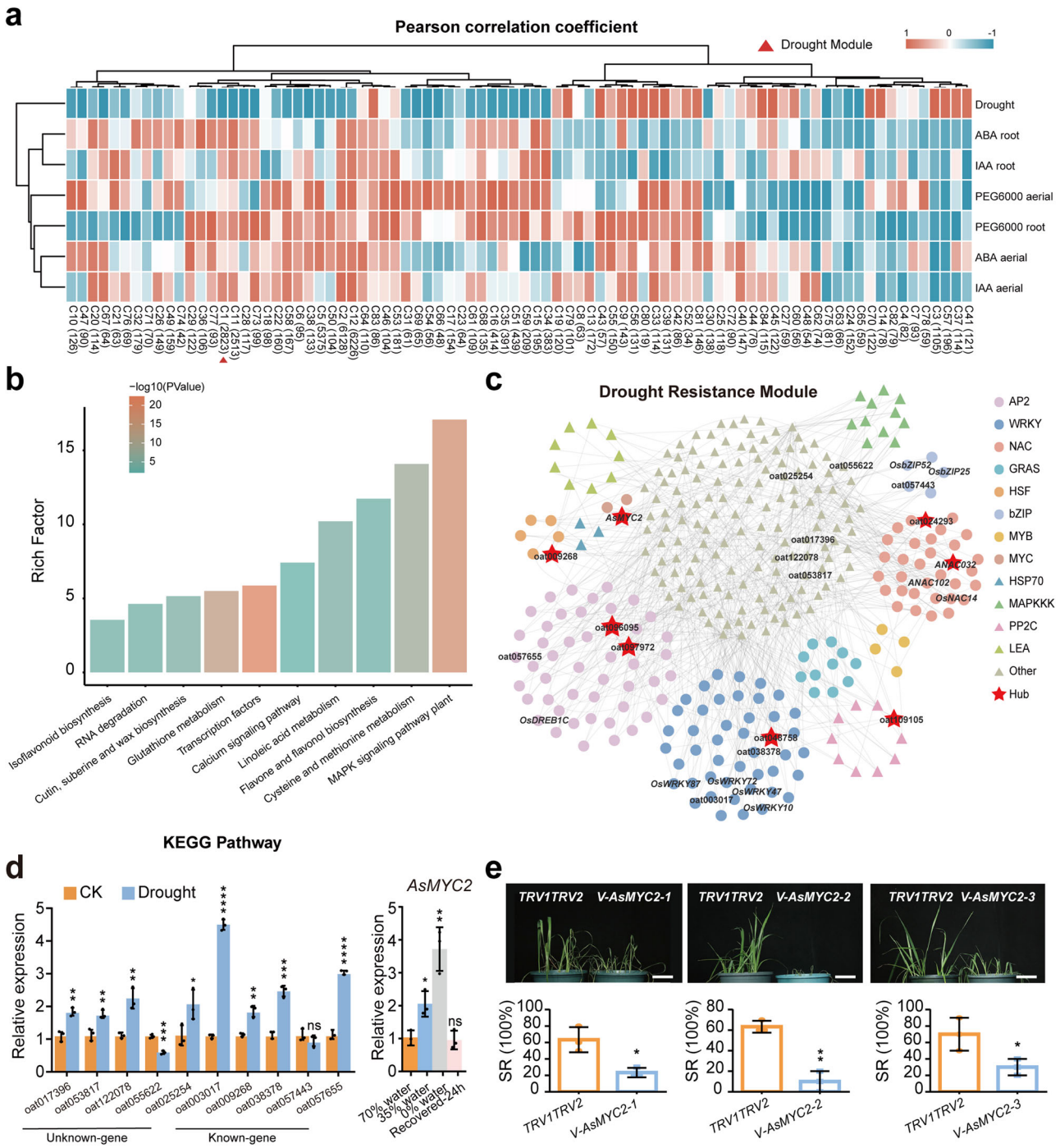

Fig. 2 | Identification of functional modules related to drought tolerance. **a** Correlation analysis between different treatments and each module. Each column represents a different cluster; for example, "C1" represents "Cluster 1". The number of genes within each cluster is indicated in parentheses. **b** KEGG analysis of differentially expressed genes in Cluster 1. **c** Drought tolerance module network. Different gene families are distinguished by color. Circles represent transcription factor genes, whereas triangles represent non-transcription factor genes. Connections illustrate gene interactions within the network. The red pentagram represents the hub transcription factor. Known drought tolerance-related genes identified in other species and potential candidate genes in oats are marked, lending credibility to the module network. **d** qRT-PCR analysis of randomly selected gene expression levels before and after drought treatment. Student's *t*-test was performed to determine statistical significance. Error bars represent the SD of three biological replicates. **e** The malfunction of *AsMYC2* decreased plant tolerance to drought. Assessment of drought tolerance of the *AsMYC2* knockdown strains. Photographs were taken after a 2-day period of recovery with full irrigation post-drought treatment. Values of survival rate statistics in the down part were means ± SD of three independent experiments; Scale bars, 5 cm. $^{*}p < 0.05$; $^{**}p < 0.01$; $^{***}p < 0.001$; $^{****}p < 0.0001$; ns, $p \geq 0.05$.

was up-regulated under drought conditions and down-regulated after rewatering (Fig. 2d). Furthermore, to investigate the effects of silencing *AsMYC2* on oat phenotypes, we used the tobacco rattle virus (TRV) VIGS system to suppress the expression of *AsMYC2* (Supplemental Fig. 5a, b). Following the successful infection by the TRV virus using the VIGS system, we obtained the following three oat lines in which *AsMYC2* was silenced: *TRV:AsMYC2-1* (*V-AsMYC2-1*), *TRV:AsMYC2-2* (*V-AsMYC2-2*) and *TRV:AsMYC2-3* (*V-AsMYC2-3*) (Supplemental Fig. 5c, d). Six-week-old oat

seedlings of *AsMYC2* knock-down lines (*V-AsMYC2*) were assessed for drought tolerance phenotype and statistical survival rate (Fig. 2e), and the *V-AsMYC2* seedlings showed decreased drought-tolerance and lower survival rate after drought treatment. These results showed that malfunctioning *AsMYC2* could lead to a decrease in plant drought tolerance, and we obtained a relatively reliable drought tolerance sub-network.

AsHSFA2c contributes to balancing drought tolerance and growth in oat

The activation of plant stress tolerance-related responses is often accompanied by energy consumption and changes in metabolic substances, with detrimental effects on growth and development. Especially, the continuous activation of stress tolerance-related responses may lead to limited plant growth and a decrease in crop yield. Therefore, there is a trade-off between plant stress tolerance and growth[52]. To mine the candidate genes involved in balancing drought tolerance and growth in oats, we identified the 'balance' modules based on the analyses of DEGs, Pearson correlation coefficient, functional enrichment, and annotated gene functions. A total of 23 modules were defined as 'balance' modules, indicating their potential roles in regulating the balance between drought tolerance and growth in oats (Supplemental Data 11). We selected Cluster 12 as a representative module to illustrate our findings (Fig. 3a) due to its high proportion of genes showing differential expression under drought-related stress (86%) and IAA treatment conditions (69%). Additionally, this cluster was highly correlated with both drought-related stress and IAA treatment (Supplemental Data 11). Functional enrichment analysis revealed that the genes in Cluster 12 were significantly associated with drought tolerance, as well as plant growth and development (Supplemental Fig. 6 and Supplemental Data 16). Notably, Cluster 12 included key genes that are known in other species for their roles in drought tolerance and growth regulation, including *OsPIL1* (oat057108)[53,54] and *OsDOG1L-2* (oat008214)[55]. Furthermore, we randomly selected 10 candidate genes from this cluster for a qRT-PCR analysis (Fig. 3b). 8 genes were responsive to both drought and IAA treatments. Among the genes in this balance module, *AsHSFA2c* (oat069028), a member of the HSF family, was identified as an ortholog of *OsHSFA2a* (Supplemental Fig. 7a, b) homologs of this gene had been previously reported to participate in the regulation of plant drought tolerance and growth[56–58]. Transcriptome and qRT-PCR data showed that the expression of *AsHSFA2c* was up-regulated by drought, as well as ABA and IAA treatments (Fig. 3c and Supplemental Fig. 8a–f). The ABA signaling pathway is the most important hormone signaling pathway in response to drought stress, whereas auxin is one of the most important hormones affecting plant growth and development. The qRT-PCR results showed that the expression of *AsHSFA2c* was significantly up-regulated after ABA and IAA treatment (Supplemental Fig. 8e, f), suggesting that the response of *AsHSFA2c* to drought stress may depend on the ABA signaling pathway and *AsHSFA2c* may affect plant growth and development via the IAA signaling pathway. Furthermore, the results of tissue-specific expression analysis showed that *AsHSFA2c* was relatively uniformly expressed across various oat tissues, with notably higher levels in flag leaves and floral organs (Supplemental Fig. 8g). The subcellular localization and nuclear-cytoplasmic separation results showed that *AsHSFA2c* was localized in the nucleus and cytoplasm (Supplemental Fig. 8h, i). These results suggest that *AsHSFA2c* may be a key molecular switch that balances drought tolerance and growth in oats.

To further investigate the function of *AsHSFA2c* in oats, we used the TRV VIGS system to suppress its expression (Fig. 3d and Supplemental Fig. 9a, b). One to three-week-old oat seedlings of *AsHSFA2c* (*V-AsHSFA2c*) knock-down lines were observed for growth phenotype and six-week-old *V-AsHSFA2c* seedlings were observed for drought-tolerance phenotype (Fig. 3e). Compared with the control, the knock-down lines of *AsHSFA2c* have been shown to be more conducive to plant growth and development, with increased chlorophyll content in leaves, heavier fresh weights, and higher plant height (Fig. 3e and Supplemental Fig. 10a–c). At the cellular level, the total number of pavement cells decreased in *V-AsHSFA2c* plants (Supplemental Fig. 10d), indicating that it may influence leaf development in oats by modulating cell division and expansion. In addition, *AsHSFA2c* knock-down plants exhibited increased sensitivity to drought (Fig. 3e and Supplemental Figs. 10a and 11a, b). The chlorophyll content, survival rate, and water loss rate were used as indicators of drought tolerance. Compared with the control, under drought conditions, *V-AsHSFA2c* had lower chlorophyll content, lower survival rate, and faster water loss rate (Supplemental Figs. 10a and 11a, b). Additionally, decreased *AsHSFA2c* expression increased the number of stomata in the lower epidermis of the leaf blade (Supplemental Fig. 10d). *AsHSFA2c* overexpression in *Arabidopsis thaliana* resulted in dwarfism and increased drought tolerance (Supplemental Fig. 12a–c), implying that in response to drought, *AsHSFA2c* expression may have regulatory effects on stomatal density. To confirm the function of *AsHSFA2c*, we used an oat genetic transformation system to generate transgenic *AsHSFA2c*-overexpressing lines (Fig. 3f–h), after which 2-week-old *AsHSFA2c*-overexpressing oat seedlings were examined in terms of growth and 4-week-old *AsHSFA2c*-overexpressing oat seedlings were observed for drought-tolerance phenotype (Fig. 3h). Compared with the control, *AsHSFA2c*-overexpressing lines have shown to be not conducive to plant growth and development while higher drought tolerance, with lower plant height (Supplemental Fig. 13a) and higher survival rate under drought treatment (Supplemental Fig. 13b). These results suggest that *AsHSFA2c* may inhibit plant growth and positively regulate drought tolerance. Collectively, we identified a module and a key candidate gene, *AsHSFA2c*, that balances drought tolerance and growth in oats.

AsDOF25 positively regulates *AsHSFA2c* as a transcription activator

To explore the upstream regulators of *AsHSFA2c* and understand how *AsHSFA2c* responds to drought stress, the nuclear run-on assay was performed. The result showed that the transcription rate of *AsHSFA2c* increased under drought conditions (Supplemental Fig. 14a). Notably, we found that a DOF transcription factor core recognition site (AAAG or CTTT) in the promoter of *AsHSFA2c* at 12-bp upstream of its translation start site (Supplemental Fig. 14b)[59]. Previous studies have shown that DOF family members participated in the regulation of plant growth and drought tolerance[60–62]. The transcriptomic analysis confirmed that most DOF family members were drought-responsive (Supplemental Fig. 14c). Therefore, we hypothesized that *AsHSFA2c* might be regulated by a DOF transcription factor. Interestingly, our co-expression network analysis revealed that 43 DOF family members were closely associated and co-expressed with *AsHSFA2c* (Fig. 4a). Among them, *AsDOF25*, a gene with close connectivity to *AsHSFA2c*, was induced by drought, ABA, and IAA treatments (Supplemental Fig. 14d–h). According to the *AsDOF25* network diagram, *AsDOF25* was correlated with HSF family genes (Supplemental Fig. 14i). Moreover, the *AsDOF25* promoter contains an ABRE binding site, which is associated with ABA signaling, and an AUXRR-core site, related to auxin response (Supplemental Fig. 14j). Thus, we hypothesized that AsDOF25 protein might bind to the *AsHSFA2c* promoter and regulate its expression. To test this hypothesis, we performed an electrophoretic mobility shift assay (EMSA) using GST-tagged AsDOF25 protein, with GST protein as a negative control (Fig. 4b and Supplemental Fig. 14k, l). The result showed that a single shifted complex was formed between the AsDOF25 protein and *AsHSFA2c* promoter, and the complex intensity decreased with the addition of the unlabeled *AsHSFA2c* promoter, but not with the mutated promoter fragment (Fig. 4b). These results indicated that AsDOF25 protein could directly bind to the promoter of *AsHSFA2c*. Subsequent experiments demonstrated that co-expressing *pAsHSFA2c::LUC* with *p35s::AsDOF25* in *Nicotiana benthamiana* leaves led to a significant increase in LUC transcript level in the co-expressed tissues compared to controls (Fig. 4c). In addition, using the TRV VIGS system, we effectively suppressed *AsDOF25* expression (Supplemental Fig. 15a, b), achieving over 50% silencing efficiency as confirmed by qRT-PCR (Supplemental Fig. 15c). The *AsHSFA2c* transcript level in *AsDOF25* mutants was significantly lower than that in control (Fig. 4d). Altogether, these results indicate that AsDOF25 protein could promote the transcription of *AsHSFA2c* as a transcription activator.

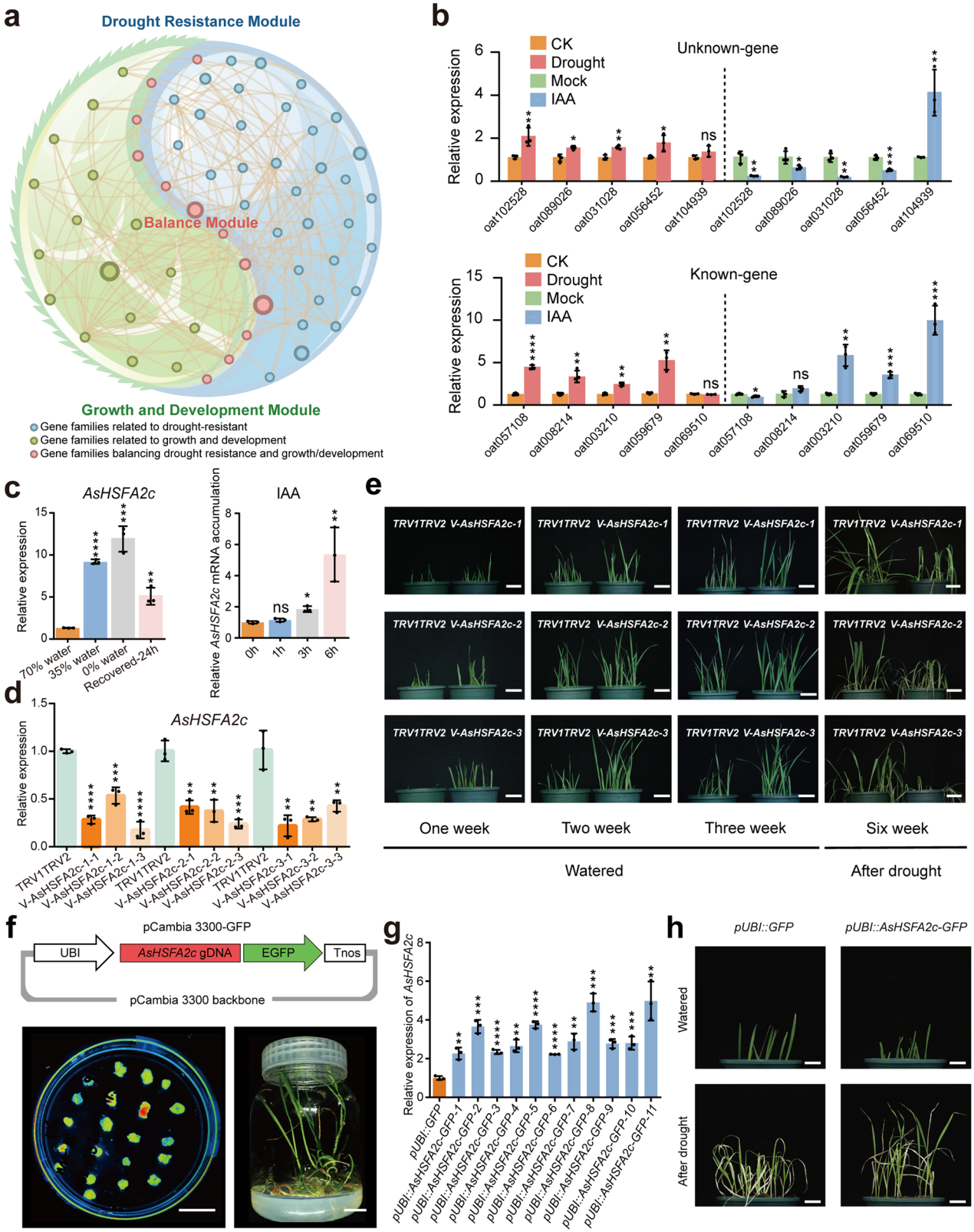

Furthermore, we also examined the roles of *AsDOF25* in plant growth and drought tolerance. Growth phenotypes of two-week-old *AsDOF25* knockdown oat seedlings (*V-AsDOF25*) were observed, and six-week-old seedlings were evaluated for drought tolerance (Fig. 4e–h). Results showed that knock-down lines for both *AsDOF25* and *AsHSFA2c* exhibited similar trends in all observed phenotypes. For example, two-week-old *V-AsDOF25* plants were taller than controls (Fig. 4e, f). Moreover, plants with *AsDOF25* malfunction showed heightened drought sensitivity (Fig. 4g), characterized by a lower survival rate and faster leaf water loss rate (Fig. 4h, i). These results indicated that *AsDOF25* inhibited plant growth and positively regulated plant drought tolerance. Therefore, we inferred that the regulation of the balance between plant growth and

Fig. 3 | Identification and verification of the balance modules and the key candidate gene, *AsHSFA2c*. **a** A schematic illustration that outlines the status of gene families identified in the 'balance' module, Cluster 12. Gene families in Cluster 12 were classified into three groups: those that play significant roles in plant growth and development (growth and development module), those crucial for drought resistance (drought resistance module), and those important for both growth and drought resistance (balance module). Each node represents a gene family, with the node size indicating the number of genes within that family. The connections between nodes represent the average correlation of co-expression between genes within the families. The green half of (**a**) represents the growth and development module, and the blue half of (**a**) represents the drought resistance module. The green nodes represent the previously reported gene families related to plant growth and development. The blue nodes represent the gene families potentially related to drought resistance. The pink nodes represent gene families potentially important for balancing drought resistance and growth/development. **b** Most of the genes in the balance module responded to both drought and IAA treatments. qRT-PCR analysis of gene expression levels before and after drought and IAA treatments. **c** *AsHSFA2c* responded to both drought and IAA treatments. **d** qRT-PCR analysis of target gene *AsHSFA2c* expression level in *AsHSFA2c* knock-down mutant lines. **e** The malfunction of *AsHSFA2c* promoted plant growth and negatively regulated plant drought tolerance. "Watered" represents well-watered conditions. "After drought" represents a 2-day period of recovery with full irrigation post-drought treatment. Scale bars, 5 cm. **f** The up part: schematic representation of the *pUBI::AsHSFA2c-GFP* vector with the Ubi promoter and Nos terminator; the down part: Detection of GFP fluorescence signal in callus induced from mature embryos infected with the *pUBI::AsHSFA2c-GFP* vector (leaf). Scale bar, 2 cm. Regeneration phenotypes of mature embryos infected with the *pUBI::AsHSFA2c-GFP* vector (right). Scale bar, 2 cm. **g** Detection of the expression of *AsHSFA2c* in the *pUBI::AsHSFA2c-GFP* genetic plants. **h** The over-expression of *AsHSFA2c* increased plant tolerance to drought. "Watered" represents well-watered conditions. "After drought" represents a 2-day period of recovery with full irrigation post-drought treatment. Scale bars, 3 cm. Student's *t*-test was performed to determine statistical significance. Error bars represent the SD of three biological replicates. $^{*}p < 0.05$; $^{**}p < 0.01$; $^{***}p < 0.001$; $^{****}p < 0.0001$; ns, $p \geq 0.05$.

drought tolerance by *AsHSFA2c* partially relied on the regulation of *AsDOF25*.

AsHSFA2c negatively regulates *AsAGO1* in balancing drought tolerance and growth in oat

A DNA affinity purification sequencing (DAP-seq) experiment was conducted to investigate the underlying mechanism by which *AsHSFA2c* balances drought tolerance and growth in oats. Following a credibility assessment of the DAP-seq peaks, we identified 1219 highly reliable peaks (Fig. 5a and Supplemental Fig. 16a). Among these peaks, 145 peaks were located within the 3 kb regions of genes, and 88 candidate genes were identified (Supplemental Data 17). To further investigate *AsHSFA2c* recognition motifs, the ±100 bp sequences flanking peaks were submitted to MEME-ChIP to search for enriched motifs (Fig. 5b). Intriguingly, among these candidate genes, the gene oat023722 (*AsAGO1*) had a significant binding signal for *AsHSFA2c* in its promoter region (Fig. 5c). The gene, *AGO1*, is a core component of the RNA-induced silencing complex (RISC) and plays a central role in the RNA silencing pathway. *AGO1* has been previously reported to regulate plant growth, development, and drought tolerance through sRNA in various species, such as *Arabidopsis thaliana* and *Oryza sativa*[63–66]. The electrophoretic mobility shift assay (EMSA) with competitive probes and mutation probes further supported that AsHSFA2c protein could bind to *AsAGO1* promoter (Fig. 5d and Supplemental Fig. 16b). Moreover, when *pAsAGO1::LUC* was co-expressed with *p35s::AsHSFA2c* in *Nicotiana benthamiana* leaves, the *LUC* transcript level was significantly lower than that in control tissues (Fig. 5e), implying that AsHSFA2c negatively regulated *AsAGO1*. The qRT-PCR results showed that the expression level of *AsAGO1* was up-regulated in *AsHSFA2c* knock-down mutants (Fig. 5f). These results indicated that *AsAGO1* was a downstream target gene of AsHSFA2c and was negatively regulated by AsHSFA2c.

To elucidate how *AsAGO1* balances growth and drought tolerance in oats, we collected plant samples exposed to drought stress and treated them with IAA for qRT-PCR analyses. The results indicated that the expression of *AsAGO1* was down-regulated by drought stress and IAA treatment in root, but up-regulated by the IAA treatment in plant aerial part (Fig. 5g, h). We subsequently used a TRV VIGS system to suppress the expression of *AsAGO1* (Fig. 5i and Supplemental Fig. 16c–e). One to three-week-old knock-down lines of *AsAGO1* (*V-AsAGO1*) were observed for growth phenotype, and six-week-old *V-AsAGO1* were observed for the drought-tolerance phenotype (Fig. 5j). Plant height, chlorophyll content, survival rate, and water loss rate were measured as phenotypic indicators (Fig. 5k-l). Under normal growth conditions, *V-AsAGO1* plants were smaller and had less chlorophyll than control plants (Fig. 5i-j). However, under drought conditions, *V-AsAGO1* lines exhibited enhanced drought tolerance, characterized by increased chlorophyll content, higher survival rate, and slower leaf water loss rate (Fig. 5j–l). These results indicated that *AsAGO1* was a downstream target gene of AsHSFA2c, and *AsAGO1* could promote plant growth and negatively regulate drought tolerance in oats.

Discussion

Drought stress is intensifying globally, posing a serious threat to food security[67]. More efforts are needed to improve the drought resistance of our major crops by identifying excellent genes related to drought tolerance. Common oat is an economically important crop worldwide, and is highly adaptable to various climatic conditions, especially drought stress[6,7]. Therefore, exploring the molecular regulatory mechanisms of the strong drought resistance in oats has become increasingly important. In this study, we constructed a genome-wide co-expression network to investigate the balance between plant growth and drought tolerance in oats, utilizing 84 transcriptome datasets from the PEG6000, drought stress, ABA, and IAA treatments (Supplemental Fig. 17a). Through in-depth data mining, we integrated networks covering various biological aspects with functional analysis tools (Supplemental Fig. 17b), and identified 23 balance modules which were significantly associated with drought tolerance, as well as plant growth and development. Many genes in these modules are involved in plant hormone signal transduction, arginine and proline metabolism, and MAPK signaling pathway (Fig. 1d), which were previously reported to be associated with plant growth and drought stress responses[68–72]. Our co-expression network and the tightly linked genes within one module may serve as a valuable resource for identifying functional genes or modules associated with growth and drought stress response, which can be used for genetic improvement and in-depth study of molecular regulatory mechanisms in oat.

HSF transcription factor family was reported to be involved in the regulation of plant growth and development and drought stress responses[16,73–77]. However, there are few reports about the regulation of HSF family members to balance between drought tolerance and plant growth. To date, the 'balancing' function of *HSFA6B* has only been reported in dryland cotton, though its molecular mechanisms and functional aspects remain insufficiently understood[78]. In this study, we uncovered the molecular mechanism of *AsHSFA2c* in balancing drought tolerance and growth in oats. Under normal conditions, as a component of the plant stress response, *AsHSFA2c* was maintained at a low expression level, which was conducive to plant growth and development. Upon drought stress, the expression of *AsHSFA2c* was upregulated, leading to an increase in plant drought tolerance. Our findings revealed that ABA and auxin reciprocally regulated the *AsDOF25-AsHSFA2c-AsAGO1* module to fine-tune the balance between drought tolerance and growth in oat, highlighting potential targets for breeding drought-tolerant oat lines. The upstream gene *AsDOF25* acts as a transcriptional activator, enhancing *AsHSFA2c* expression, whereas *AsHSFA2c*, acting as a transcriptional repressor, suppresses the downstream target gene *AsAGO1* (Supplemental Fig. 17c). We found that 2273 DEGs were co-expressed with the

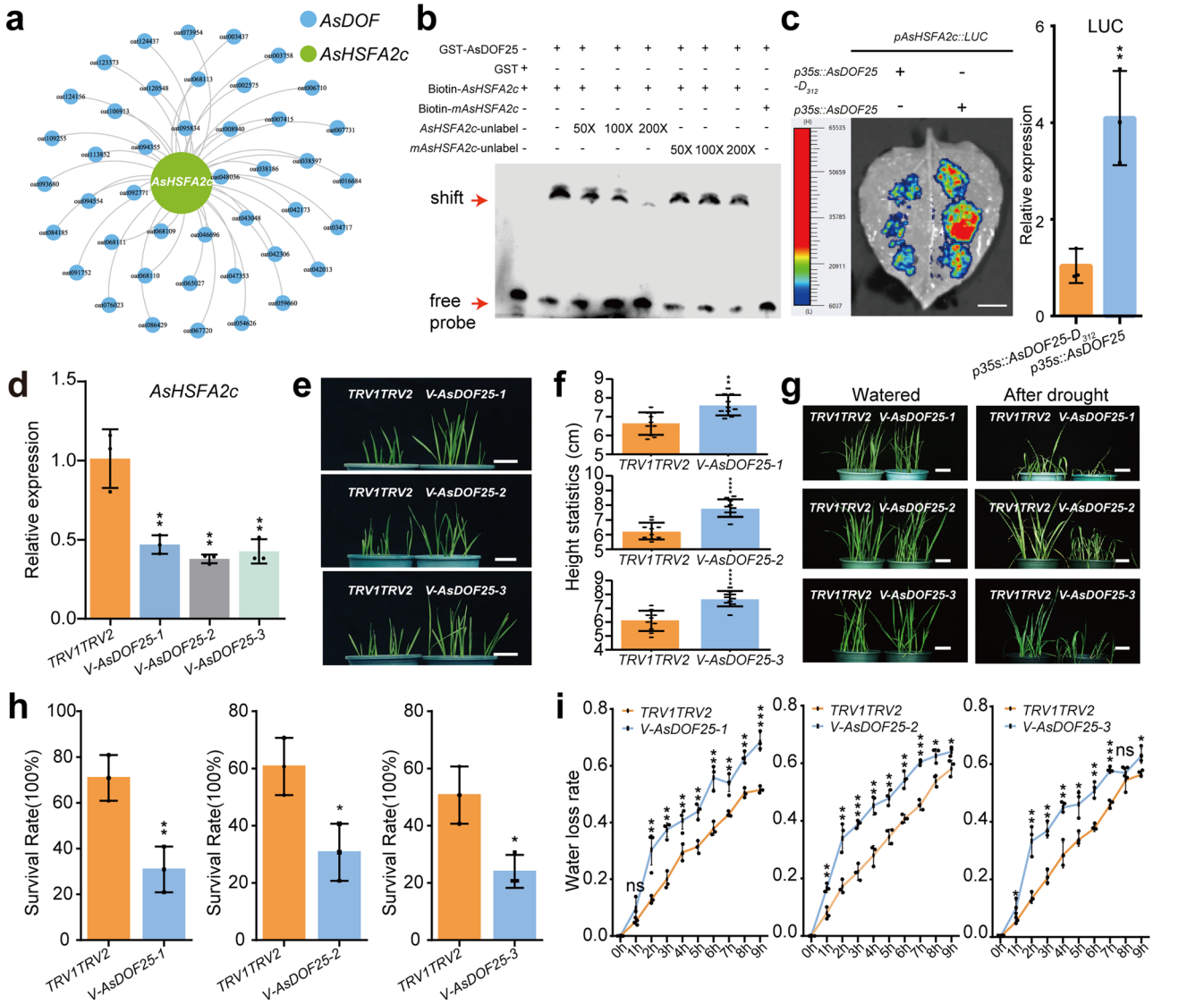

Fig. 4 | AsDOF25 positively regulates *AsHSFA2c* via transcription activation. a A circular gene network diagram was displayed, with *AsHSFA2c* as the core, surrounded by genes associated with *AsDOF* family members, and gene connections represented connectivity. **b** EMSA assay showed that AsDOF25 protein bound the promoter of *AsHSFA2c*. GST-AsDOF25 was incubated with 5′-biotin-labeled DNA probes with *AsHSFA2c* promoter sequence (Biotin-*AsHSFA2c*) or mutated *AsHSFA2c* promoter sequence (Biotin-*mAsHSFA2c*). **c** Luciferase assay showed that AsDOF25 activated the *AsHSFA2c* promoter. *N.benthamiana* plants were co-inoculated with *p35s::AsDOF25-D*$_{312}$/*p35s::AsDOF25* and *pAsHSFA2c::LUC*. The *p35s::AsDOF25-D*$_{312}$ plasmid contains only the transcriptional binding domain of *AsDOF25* and lacks its transcriptional activation domain. The sample was collected at 48 hpi. A cooled CCD imaging apparatus (Roper Scientific) was used to capture luciferase images. Scale bar, 0.5 cm. qRT-PCR detection of LUC expression level. *N.benthamiana* plants were co-inoculated with *p35s::AsDOF25-D*$_{312}$ and *pAsHSFA2c::LUC* as a negative control. **d** qRT-PCR detection of *AsHSFA2c* expression level in *AsDOF25* knock-down mutants. Two-leaves-stage plant samples were collected. **e**, **f** The malfunction of *AsDOF25* promoted the growth of plants. Whole-plant images of 2-week-old plants (**e**). Scale bars, 5 cm. Statistical analyses of plant height are presented in panel (**f**), $n = 10$. **g**, **h** Drought tolerance assessment of *AsDOF25* knockdown lines. Photographs were taken under well-watered conditions and after a 2-day period of recovery with full irrigation post-drought treatment. Whole-plant images of 5-week-old plants (**g**). Scale bars, 5 cm. Values in (**h**) were means ± SD from three independent experiments. **i** Water loss rate statistics of *AsDOF25* knock-down strains. The error bar represents the SD of three biological replicates. *$p < 0.05$; **$p < 0.01$; ***$p < 0.001$; ****$p < 0.0001$; ns, $p \geq 0.05$.

AsDOF25-AsHSFA2c-AsAGO1 module in response to drought and PEG6000 treatments. Additionally, we found that under IAA treatments, the expression of *AsAGO1* showed opposite expression trends in different tissues (Fig. 5h), which is similar to previous reports in rice that under IAA treatment, the expression trends of *OsAGO1b* (Os04g0566500) showed inconsistency in buds and roots[79]. So far, the underlying causes of this phenomenon remain unclear. AGO protein is a core member of the ISC complex in RNA silencing signaling pathway[80], which regulates the function of target genes by loading sRNA. When *AsAGO1* is induced, the expression of many sRNAs and its target genes will change. Therefore, we proposed that the response of *AsAGO1* to IAA, along with its influence on growth and development, was likely a complex process that may not be regulated by a single factor.

When drought stress comes, specific receptors on the plasma membrane of plant cells perceive the drought signal, including G protein-coupled receptors (GPCRs)[81], receptor-like kinases (RLKs)[82], histidine kinases (HKs)[83], abscisic acid (ABA) receptors[84] and calcium-sensing receptors(CAS)[85]. Subsequently, several secondary messengers are generated within the cell, which in turn activate downstream signal transduction pathways, including the ABA-mediated signaling pathway, Ca^{2+}-activated CBL-CIPK signaling pathway, and MAPK cascade signaling pathway[86–89]. Among them, the ABA-mediated signal transduction pathway is considered

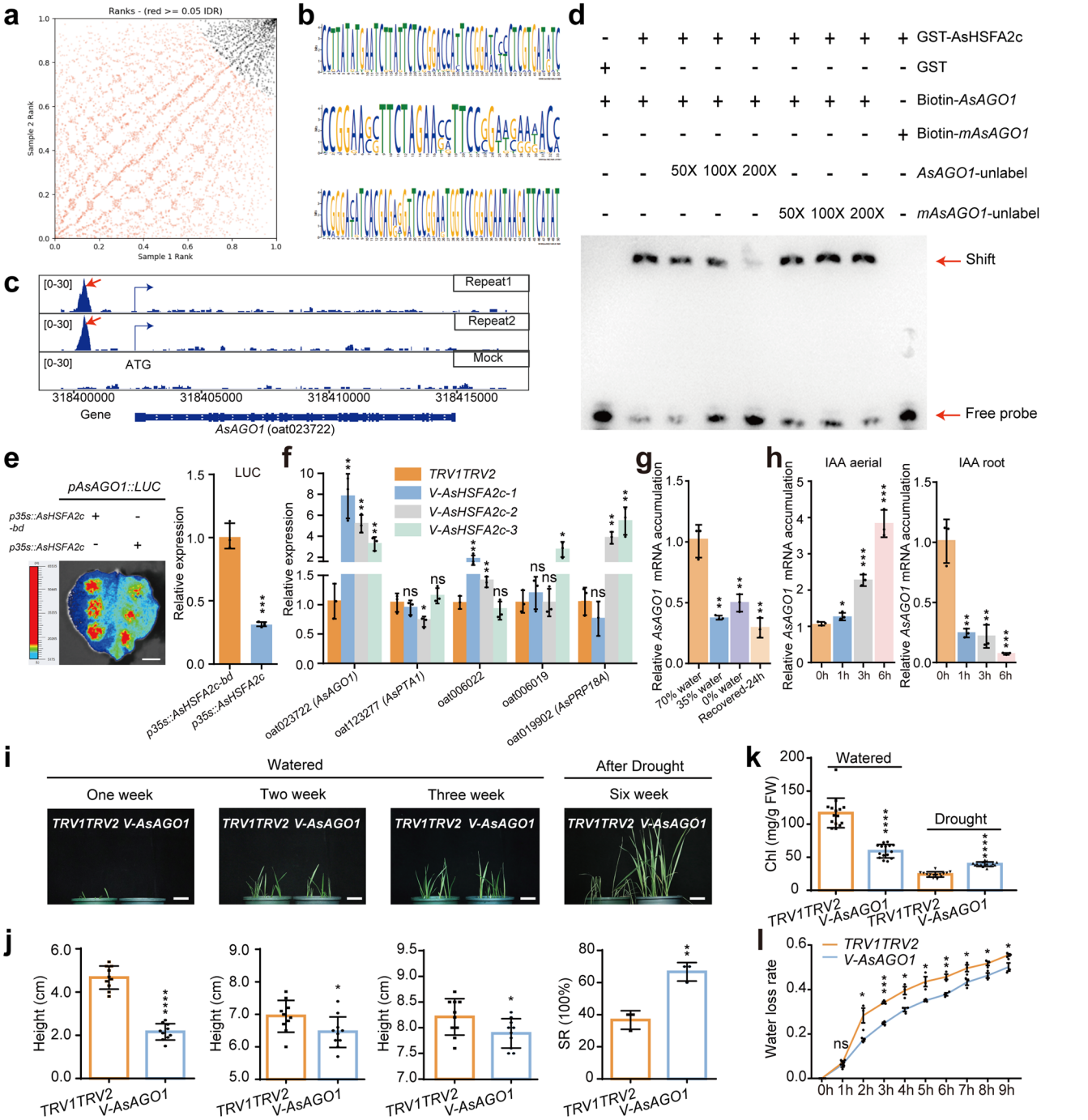

Fig. 5 | AsHSFA2c negatively regulates *AsAGO1* through transcriptional inhibition. a The credibility evaluation of DAP-seq peaks showed that peaks below the IDR threshold were displayed in red (non-reproducible peaks), and peaks above were displayed in black (biologically reproducible peaks). **b** Three different secondary position weight matrices (PWM) represented the obtained motifs in the experiment, with a *Z* score indicated. **c** A significant binding signal of *AsHSFA2c* was identified in the *AsAGO1* promoter by DAP-seq. **d** EMSA assay showed that AsHSFA2c protein bound the promoter of *AsAGO1*. GST-AsHSFA2c was incubated with 5′-biotin-labeled DNA probes with *AsAGO1* promoter sequence (Biotin-*AsAGO1*) or mutated *AsAGO1* promoter sequence (Biotin-*mAsAGO1*). **e** Luciferase assay showed that *AsHSFA2c* inhibited the *AsAGO1* promoter. *N.benthamiana* plants were co-inoculated with *p35s::AsHSFA2c-bd*/*p35s::AsHSFA2c* and *pAsAGO1::LUC*. The *p35s::AsHSFA2c-bd* plasmid contains only the transcriptional binding domain of *AsHSFA2c* and lacks its transcriptional activation domain. The sample was collected at 48 hpi. A cooled CCD imaging apparatus (Roper Scientific) was used to capture luciferase images. Scale bar, 0.5 cm. qRT-PCR detection of LUC expression level. *N.benthamiana* plants were co-inoculated with *p35s::AsHSFA2c-bd* and *pAsAGO1::LUC* as a negative control. Error bars represent the SD of three biological replicates. **f** Relative expression of genes selected from DAP-seq in *TRV1TRV2* and *AsHSFA2c* knockdown lines. Error bars represent the SD of three biological replicates. **g**, **h** qRT-PCR detection of *AsAGO1* expression level under drought (**g**) and IAA treatment (**h**). The *X*-axis represents processing time. Error bars represent the SD of three biological replicates. **i**, **j** The malfunction of *AsAGO1* inhibited plant growth and positively regulated plant drought tolerance. "Watered" represented well-watered conditions. "After Drought" represented a 2-day period of recovery with full irrigation post-drought treatment (**i**). Scale bars, 5 cm. Statistics on plant height (error bars represent the SD of 15 biological replicates) and survival rate (error bars represent the SD of three biological replicates) of *AsAGO1* knock-down strains (**j**). **k** Chlorophyll contents detection statistics of *AsAGO1* knockdown lines. Error bars represent the SD of 15 biological replicates. **l** Water loss rate statistics of *AsAGO1* knock-down lines. Error bars represent the SD of three biological replicates. Student's *t*-test was performed to determine statistical significance. $^{*}p < 0.05$; $^{**}p < 0.01$; $^{***}p < 0.001$; $^{****}p < 0.0001$; ns, $p \geq 0.05$.

to be the main pathway mediating plants' response to drought stress[90]. Specifically, the signaling receptor PYR/PYL/RCAR protein complex binds to PP2Cs (phosphatase type 2Cs) and inhibits the activity of PP2Cs, thereby activating the phosphorylation activity of SnRK2s (phosphatsenon-fermenting SNF1-related protein Kinase2s). Finally, a series of downstream ABA signaling pathway response factors are activated to strengthen plant resistance to drought stress[1]. Previous studies have shown that DOF family genes are responsive to the ABA signaling pathway[91–94]. However, the role of DOF family genes in drought response via ABA signaling has not been reported. In this study, we found that the expression of *AsDOF25* was up-regulated after ABA treatment (Supplemental Fig. 14e, f), and *AsDOF25* was correlated with the ABA receptor PYR/PYL/RCAR protein complex in the co-expression network (Supplemental Fig. 14i). Furthermore, we also identified an ABRE motif in the *AsDOF25* promoter region (Supplemental Fig. 14j). ABA generally regulates target gene expression through transcription factors known as ABRE-binding protein/ABRE-binding factors (AREB/ABF)[95–97]. These results suggest that *AsDOF25* may respond to drought stress via the ABA signaling pathway. However, more evidence is needed to support this hypothesis.

Both DOF and HSF family genes are involved in regulating plant growth and development in response to IAA signals[98–101], while also regulating plant drought tolerance through ABA signaling pathways[94,102–104]. Our results further demonstrated the role of the *AsDOF25-AsHSFA2c-AsAGO1* module in fine-tuning the balance between plant growth and drought tolerance. Unexpectedly, the expression levels of *AsDOF25* and *AsHSFA2c* were up-regulated after IAA treatment, whereas a plant-enlarged phenotype was observed after the malfunction of *AsDOF25* and *AsHSFA2c* (Figs. 3c, e, and 4e and Supplemental Fig. 14g, h). We hypothesized that this might be due to the expression of other plant growth-promoting genes downstream of the *AsDOF25-AsHSFA2c* module (Supplemental Fig. 18a–d). For example, the candidate downstream genes targeted by AsHSFA2c, namely oat043386 and oat123997, which were identified on DAP-seq, may be transcriptional repression by AsHSFA2c (Supplemental Fig. 18c, d), have homologs in rice (*OsGAE1* and *OsVTE5*, respectively). Previous studies have shown that they play a positive regulatory role in promoting plant growth and development[105,106]. Meanwhile, we evaluated the impact of the IAA concentration used in the experiment on oat growth and found that its growth was notably suppressed at 2 days after IAA treatment (Supplemental Fig. 19). Therefore, we hypothesize that this also may be associated with the high concentration of IAA treatment.

Furthermore, it is generally expected that IAA (a growth-promoting hormone) and drought stress would induce opposite gene expression patterns while our results showed that the expression levels of *AsDOF25* and *AsHSFA2c* were up-regulated after both IAA and drought treatments. Previous studies have reported that there exists complex crosstalk among various signaling pathways that regulate growth and development, as well as responses to biotic and abiotic stresses in plant[107–111]. Our transcriptome data revealed that most of genes exhibited opposite expression trends under IAA and drought treatments (Supplemental Fig. 2d). Conversely, a portion of genes exhibited similar expression patterns following drought and IAA treatments (Supplemental Fig. 2d). This may be because that plants also can actively respond drought stress by up-regulating the expression of growth-related genes[9], such as the previously reported genes *TaIAA15-1A*, *RRS1*, *TrIAA27*, *SOT17*[112–115], or that exogenous IAA treatment significantly increased ABA and jasmonic acid (JA) content, leading to the up-regulated expression of drought stress-responsive genes, such as *bZIP11*, *DREB2*, *MYB14*, *MYB48*, *WRKY2*, *WRKY56*, *WRKY108*, and *RD22*[116].

Methods

Plant materials, growth conditions, and treatments

Avena sativa (*A. sativa*; oat) plants were grown in a greenhouse at 25 °C/18 °C under a 16-h light/8-h dark photoperiod. *N. benthamiana* and *A. thaliana* plants were grown at 22 °C under a 12-h light/12-h dark photoperiod. 'cv. Mengyan No.1' was obtained from Inner Mongolia Agricultural University. To generate transgenic *Arabidopsis thaliana* plants overexpressing *AsHSFA2c*, the *p35S::oat069028* (*AsHSFA2c*) was transformed into Col-0. To generate transgenic *Avena sativa* plants overexpressing *AsHSFA2c*, the *pUBI::oat069028* (*AsHSFA2c*)*-GFP* was transformed into 'cv. Bayou No.18'.

To initiate the experiment, seeds of 'cv. Mengyan No.1' and 'cv. Bayou No.3' were immersed in 75% ethyl alcohol for 3 min, and then in a 10% (*w*/*v*) sodium hypochlorite (NaClO) solution for 20 min. The seeds were washed four times with sterilized deionized water and then vernalized for 3 days at 4 °C under shaded light conditions. Seeds of *N. benthamiana* and *A. thaliana*, using a 75% ethyl alcohol for 2 min, a 3% (*w*/*v*) sodium hypochlorite (NaClO) solution for 10 min, were washed four times with sterilized deionized water and then vernalized for 3 days at 4 °C under shaded light conditions. Seeds of *N. benthamiana* and *A. thaliana* were immersed in 75% ethyl alcohol for 2 min, and then in 3% (*w*/*v*) sodium hypochlorite (NaClO) solution for 10 min. The seeds were washed four times with sterilized deionized water and then vernalized for 3 days at 4 °C under shaded light conditions.

Sterilized seeds were carefully placed on 1/2 MS medium supplemented with 1% (*w*/*v*) agar and adjusted to pH = 5.8. Germinated seeds were transferred to pots filled with 1/2 Hoagland solution, which was refreshed every 2 days. When the seedlings reached the trifoliate stage, they were subjected to the following four treatments: drought, ABA (spraying and soaking), IAA (spraying and soaking), and 20% PEG6000 solution (simulated drought). Whole plants were collected at specific time points after initiating the drought treatment [70% soil moisture content (watered, 0 day after treatment), 35% soil moisture content (moderate drought, 4 days after treatment), 0% soil moisture content (severe drought, 10 days after treatment), and recovered-24h]. Treatments were completed using solutions containing 20% PEG6000 to simulate drought conditions. Plant aerial parts and roots were collected at specific time points (0 h, 6 h, and 12 h) after initiating the PEG6000 treatment. Hormone treatments involved the following solutions: 250 μmol L^{-1} (spraying)/125 μmol L^{-1} (soaking) ABA and 250 μmol L^{-1} (spraying)/125 μmol L^{-1} (soaking) IAA. Plant aerial parts and roots were collected at specific time points (0 h, 1 h, 3 h, 6 h, and 9 h) after initiating the ABA and IAA treatments.

For plant organ-specific expression analysis, 'cv. Mengyan No. 1' plants were grown in pots and then various tissue samples were collected from various plant parts, including roots, stems, leaves, flag leaves, flowers, pods, and seeds.

RNA sequencing

Tissues from the roots and the plant aerial parts of plants treated with ABA, IAA, and PEG6000, as well as whole plants that underwent the drought treatment were collected for transcriptome sequencing. The tissue samples were frozen in liquid nitrogen and stored at −80 °C. Three biological replicates were collected for each tissue sample. Total RNA was extracted from the tissue samples using an RNeasy Plant Mini Kit (Qiagen). cDNA library was constructed by VAHTS Universal V6 RNA-seq Library Prep kit for Illumina (Vazyme, NR604-01). The mRNA of eukaryotic cells is enriched using Oligo (dT) magnetic beads and then fragmented by adding Fragmentation Buffer. Using mRNA as a template, a first-strand cDNA is synthesized with hexamer random primers. Then, with the addition of dNTPs, DNA polymerase I, and RNase H, the second-strand cDNA is synthesized. Purified double-stranded cDNA undergoes end repair, addition of an A-base, ligation of sequencing adapters, and fragment selection to recover cDNA fragments of approximately 350 bp. Finally, PCR enrichment to obtain the cDNA library, and paired-end sequencing was performed on a NovaSeq sequencing platform (Illumina) (Annoroad Gene Technology, Beijing, China).

Transcriptome analysis

The sequenced reads were trimmed by Fastp (Version: 0.20.1). Clean RNA-seq reads from the 84 samples were mapped to the 'cv. Pinyan No.6' genome by HISAT2 (version: 2.2.1)[117]. Gene expression levels were calculated in terms of the fragments per kilobase of exon per million mapped fragments (FPKM) value using StringTie (version: 2.1.6)[118] with the parameter "-G -e

-A". Differentially expressed genes were identified using the DESeq2 R package (version:1.38.3), with default parameters. We filtered the DEGs with a minimum of two-fold differential expression (|fold change| ≥ 2; false discovery rate (FDR) ≤ 0.05;) and with the FPKM value higher than 1.

Identify genes involved in the ABA and IAA signaling pathways in oat

To identify genes involved in the ABA and IAA signaling pathways in oats, we first utilized the Rice Annotation Project Database (RAP-DB, http://rapdb.dna.affrc.go.jp/) to gather genes that have been previously identified as key components of the ABA and IAA signaling pathways. Subsequently, we utilized JCVI (version: 1.2.1) to construct the gene collinearity between rice and oat, identifying orthologous genes of rice in the oat genome. Based on annotations from RAP-DB, we then determined the members of the ABA and IAA signaling pathways in oats.

GO and KEGG enrichment analysis

Genes annotated with GO terms in the 'cv. Pinyan No. 6' genome annotated to 124,604 genes was considered as the background. The GO terms and KEGG pathways are assigned to the genes in 'cv. Pinyan No.6' were retrieved from the corresponding InterPro entry. GO and KEGG enrichment analyses were performed using the R package clusterProfiler. The resulting p values were corrected according to Benjamini and Hochberg's method. GO terms and KEGG pathways with an adjusted p values < 0.05 were considered to be significantly enriched.

Construction of co-expression networks

To comprehensively evaluate the co-expression relationships among genes during drought response and growth in oats, gene expression levels were first calculated for the 84 transcriptome data for the different treatments associated with growth and drought tolerance in oats to obtain the fragments per kilobase of exon per million mapped fragments (FPKM) using StringTie (version 2.1.6)[118] with the parameters -G -e -A. Then, differentially expressed genes (DEGs) were identified using the R package of DESeq2 (version 1.38.3) with the parameters of a minimum two-fold change in expression (FPKM > 0.1; |fold-change| ≥ 2; false discovery rate (FDR) ≤ 0.05)[4]. Next, we applied the R package of WGCNA to obtain the genes that were expressed in at least three samples (goodSamplesGenes (datExpr, verbose = 3))[119,120], and the co-expression network was constructed using 33,611 DEGs that met the criteria of FPKM > 0.1, a two-fold expression change between control and treatment, and a topological overlap value > 0.3. Cytoscape (version: 3.10.1) and Gephi (version: 0.10) were used to visualize the network and to extract network subsets.

Definition of the 'balance' module

To identify candidate modules involved in balancing drought tolerance and growth in oats, four conditions were required. First, more than 5% of the genes in the module were differentially expressed both in IAA-treated and drought-treated conditions. Second, based on the correlation analysis between different treatments and the modules, we identified the modules that were highly correlated with both of IAA and drought treatment, and the Pearson correlation coefficient is >0.8 for both IAA treatment and drought treatment. Third, gene functional enrichment analysis for each module was performed, and the modules with the functional enrichment items covering both of drought-related and growth-related items were defined as the candidate 'balance' modules. Additionally, the module, harboring key genes that have been previously reported to play important roles in plant development and drought tolerance, was also defined as the candidate 'balance' module. Finally, the modules that meet all the bove four conditions were defined as the 'balance' modules.

Correlation analysis

The Pearson correlation analysis was conducted to assess the correlation between gene modules and treatments[121,122]. According to a Spearman correlation analysis, the degree of correlation between gene modules and treatments was determined on the basis of the correlation coefficient "r" ($|r| > 0.8$).

Gene family identification

HSF gene sequences were extracted from the 'cv Pinyan No.6' genome and then compared with HSF gene sequences from the *O. sativa* genome by BLAST and retrieved by HMMER (version: 3.4).

Phylogenetic analysis

To explore the phylogenetic relationships of the HSF gene family in *A. sativa*, we constructed phylogenetic trees comprising HSF genes from *A. sativa*, *T. aestivum*, and *O. sativa*. Three subclasses were assigned according to the relationships of HSF gene family members in *O. sativa* (https://ricedata.cn/). The phylogenetic tree of the HSF gene families was constructed using iqtree (version: 2.2.2.7)[123]. The website iTOL was used for the visualization of the phylogenetic tree[124].

DAP-seq

DAP-seq was performed at Bluescape Hebei Biotech[125–128] to purify gDNA from the leaves of *Avena sativa*. Genomic DNA (gDNA, 5 μg in 130 μL TE buffer) was extracted using the CTAB (Sangon Biotech, A600108) and fragmented to an average of 200 bp using a Covaris M220 (Woburn, MA, USA). A genomic DNA library was prepared using a DNA Affinity Purification Sequencing Kit (Bluescape Hebei Biotech Co., Ltd.). *AsHSFA2c* was fused to the Halo affinity tag and expressed using the TNT SP6 Coupled Wheat Germ Protein Expression System (Bluescape, Hebei, China) for expression in a 50 μL reaction with a 2 h incubation at 37 °C. AsHSFA2c protein and the gDNA library were incubated in vitro and DNA bound to AsHSFA2c protein was isolated by the HaloTag beads (Promega)[71,129].

To significantly decrease or eliminate false peak signals, the input DNA was used as a negative control sample for background reference. Two biological replicates were conducted for the experiment. DNA obtained through affinity purification and elution was subjected to paired-end sequencing using an Illumina HiSeq platform, with quality-filtered reads aligned to the 'cv. Pinyan No.6' genome sequence using BWA. In addition, peak calling was performed by MACS2[130], whereas the irreproducibility discovery rate (IDR) method was used to obtain highly reproducible peaks (IDR < 0.05) (https://github.com/nboley/idr)[131]. Then we retained the peaks overlapping the 3 kb regions upstream and downstream of genes for the subsequent analysis. Finally, motifs were identified using the Simple MEME Wrapper function model of TBtools[132].

Synteny analysis

Genome-wide synteny analysis between *A. sativa* and *O. sativa*. was conducted using JCVI (Version: 1.2.1) with the default parameters.

Virus-induced gene silencing mediated by TRV

Agrobacterium tumefaciens strain GV3101 with the tobacco rattle virus (TRV) full-length infectious clone TRV was cultured at 28 °C in LB medium containing 25 μg mL^{-1} rifampicin, and 25 μg mL^{-1} kanamycin.

To investigate the potential role of *AsMYC2, AsHSFA2c, AsDOF25,* and *AsAGO1* in drought tolerance and growth of oats, we employed the Tobacco Rattle Virus (TRV) virus-induced gene silencing (VIGS) system to knock down the expression of these genes. Three fragments of different lengths within these gene ORFs, namely *V-AsMYC2-1*, *V-AsMYC2-2*, *V-AsMYC2-3*, *V-AsHSFA2c-1*, *V-AsHSFA2c-2*, *V-AsHSFA2c-3*, *V-AsDOF25-1*, *V-AsDOF25-2*, *V-AsDOF25-3*, *V-AsAGO1-1* were selected for these purposes. These fragments were subcloned into the TRV2 infection plasmid vector using an NC clone (NC Biotech). To initiate the virus-induced gene silencing assay, *A. tumefaciens* strains GV3101 carrying pTRV1 and different pTRV2 derived vectors (TRV2, *V-AsMYC2*, *V-AsHSFA2c*, *V-AsDOF25*, and *V-AsAGO1*) in a 1:1 ratio were mixed in medium supplemented with acetosyringone (AS) (19.62 mg L^{-1}), cysteine (Cys) (400 mg L^{-1}), and Tween-20 (5 mL L^{-1}). The infection experiment conditions were set to 20 kPa vacuum infiltration for 5 min[133]. And then, co-

cultured overnight at 28 °C with shaking at 180 rpm. After co-cultivation, the Agrobacterium-infected (germinated) seeds were washed with sterile water to remove surface-adhered Agrobacterium. Finally, these seeds were planted in the soil.

Plasmids and cloning procedures

To generate entry constructs, the different lengths ORF fragment regions of *AsMYC2*, *AsHSFA2c*, *AsDOF25*, and *AsAGO1* were amplified from 'cv. Mengyan No.1' cDNA. These fragments were then cloned into the TRV2 infection plasmid vector using NC clone (NC Biotech) to generate the following constructs: *pTRV2::AsMYC2-1*, *pTRV2::AsMYC2-2*, *pTRV2::AsMYC2-3*, *pTRV2::AsHSFA2c-1*, *pTRV2::AsHSFA2c-2*, *pTRV2::AsHSFA2c-3*, *pTRV2::AsDOF25-1*, *pTRV2::AsDOF25-2*, *pTRV2::AsDOF25-3*, and *pTRV2::AsAGO1*.

A 3,218-bp genomic DNA fragment containing the *AsHSFA2c* promoter and genic sequence was cloned into *pCambia1305-GFP* using the ClonExpressII One Step Cloning Kits (Vazyme, Nanjing, China) to generate the *pAsHSFA2c::AsHSFA2c-GFP* construct. The full-length CDS region of *AsHSFA2c* was cloned into *pCambia3300-GFP* using the ClonExpressII One Step Cloning Kits to generate the *pUBI::AsHSFA2c-GFP* construct. A 2,000-bp genomic DNA fragment containing the *AsHSFA2c* promoter sequence was cloned into *pNC-Green-LUC* using the NC clone mix (NC Biotech) to generate the *pAsHSFA2c::LUC* construct. A 3,000-bp genomic DNA fragment containing the *AsAGO1* promoter sequence was cloned into *pNC-Green-LUC* using the NC clone mix (NC Biotech) to generate the *pAsAGO1::LUC* construct.

The full-length CDS region of *AsDOF25* and a 936-bp DNA fragment containing 1-312 amino acids from *AsDOF25* were amplified from 'cv. Mengyan No.1' cDNA, these fragments were then cloned into *pCambia3304* (containing GFP tag, not fused with the target gene) with NC clone mix (NC Biotech) to generate *p35s::AsDOF25* and *p35s::AsDOF25-D_{312}* constructs. The full-length CDS region of *AsHSFA2c* was amplified from 'cv. Mengyan No.1' cDNA, these fragments were cloned into *pCambia3304* with NC clone mix (NC Biotech) to generate *p35s::AsHSFA2c* constructs. A 438-bp DNA fragment containing 1-146 amino acids from *AsHSFA2c* was amplified from 'cv Mengyan No.1' cDNA, the fragments were then cloned into *pCambia3304* with NC clone mix (NC Biotech) to generate *p35s::AsHSFA2c-bd* constructs.

For prokaryotic expression, the *pGEX4T-1-GST-AsDOF25* construct was generated by inserting *AsDOF25* full-length CDS into pGEX4T-1 digested with BamHI and EcoRI. *pGEX4T-1-GST-AsHSFA2c* construct was generated by inserting *AsHSFA2c* full-length CDS into *pGEX4T-1* digested with BamHI and EcoRI. All primers are listed in Supplemental Data 18.

Luciferase assay

For *AsDOF25* activitied *AsHSFA2c* promoter activity assay, *A. tumefaciens* GV3101 strain carrying *p35s::AsDOF25* and *pAsHSFA2c::LUC* constructs were co-infiltrated into the leaves of 4-week-old *N. benthamiana* plants. Two days after infiltration, plant samples were collected to detect fluorescence due to luciferase activity and conduct a qRT-PCR analysis. The *p35s::AsDOF25-D_{312}* construct was used as a negative control. For *AsHSFA2c* inhibited *AsAGO1* promoter activity assay, *A. tumefaciens* GV3101 strain carrying *p35s::AsHSFA2c* and *pAsAGO1::LUC* constructs were co-infiltrated into leaves of 4-week-old *N. benthamiana* plants. Two days after infiltration, plant samples were collected to detect fluorescence due to luciferase activity and conduct a qRT-PCR analysis. The *p35s::AsHSFA2c-bd* construct was used as a negative control.

Reverse transcription PCR analysis

Total RNA was extracted with TRIzol reagent (Thermo Fisher Scientific). 1 μg total RNA was converted to cDNA with the PrimeScript RT Reagent Kit (Takara, RR047A), and the RT-qPCR was performed with a TB Green Premix Ex Taq kit (Tli RNase H Plus) (Takara, R420A). *AsACT2* was used as an internal control. All primers used in the RT-qPCR assays are listed in Supplemental Data 18.

Genetic transformation in *Avena sativa*

Mature embryos of healthy 'cv. Bayou No.18' plants grown in a well-conditioned greenhouse were collected and cultured on L3-M medium (4.6 g L^{-1} L3 base salts with vitamins, 30 g L^{-1} maltose, 4 g L^{-1} phytagel, 2 g L^{-1} 2,4-D, 1 g L^{-1} dicamba) until embryonic calli were produced[134]. *Agrobacterium tumefaciens* strain GV3101 with *pUBI::AsHSFA2c-GFP* was cultured at 28 °C in YEP medium overnight. After centrifugation at 25 °C and 5,000 rpm for 10 min, the precipitate was resuspended in WLS solution (pH 5.8) consisting of 4.30 g Linsmaise & Skoog Base Salts, 100 μL 1000 × MS vitamins, 10 g glucose, and 0.5 g MES (per liter of H_2O) for an optical density (OD) of 0.5[135]. Embryonic calli were immersed in a mixture comprising equal proportions of *A. tumefaciens* GV3101 cells containing *pUBI::AsHSFA2c-GFP* and *A. tumefaciens* GV3101 cells containing *pUBI::TaWOX5* for 30 min. Then, the embryogenic callus was removed, and the residual bacterial liquid was absorbed using filter paper. Embryonic calli were collected, after which the residual bacterial mixture was absorbed using filter paper and the embryonic calli were cultured on filter paper containing 75 μmol acetosyringone in darkness for 3 days. Next, embryonic calli were cultured on WLS-RES medium (4.6 g L^{-1} L3 base salts with vitamins, 2.2 mg L^{-1} Picloram, 0.5 g L^{-1} glutamic acid, 0.1 g L^{-1} Casein acid Hydrolysate, 0.75 g L^{-1} $MgCl_2 \cdot 6H_2O$, 40 g L^{-1} Maltose, 1.95 g L^{-1} MES, 4 g L^{-1} phytagel, 0.5 mg L^{-1} 2,4-D, 0.85 mg L^{-1} $AgNO_3$, 0.1 mg L^{-1} Ascorbic Acid, 0.2 g L^{-1} Timentin, PH 5.8) for 5 days. WLS-P5 medium (the wls-res medium containing 0.5–5 mg L^{-1} Basta) was used for gradient screening, with surviving calli transferred to regeneration medium (pH 5.8) comprising 4.6 g L3 base salts with vitamins, 5 mg zeatin, 20 g sucrose, 0.5 g MES, 200 μL 12.5 g L^{-1} $CuSO_4 \cdot 5H_2O$, and 4 g phytagel (per liter of H_2O)[136,137]. The calli were grown until they reached a size of 3–5 cm. Finally, the roots were cultured in a rooting medium (pH 5.8) comprising 4.6 g L3 base salts with vitamins, 0.2 mg L^{-1} IBA, 15 g sucrose, 0.5 g MES, and 4 g phytagel (per liter of H_2O). *AsHSFA2c* expression was analyzed by qRT-PCR.

Drought phenotype analyses

For drought phenotype analyses of oats at the seedling stage, ten seedlings were planted in one pot with a soil mixture. The seedlings were fully watered at the trifoliate stage and then stopped water supply until the gene knockdown lines/ the gene overexpression lines had different leaf wilting phenotypes compared with the negative control line (*TRV1TRV2/ pUBI::GFP* transgenic lines). Photographs were taken after a 2-day period of recovery with full irrigation post-drought treatment. Survival rates were recorded after rewatering for 2 days.

Water loss rate analyses

The seedlings were grown until the second leaf totally expanded under well-watered conditions. The leaves were taken from six plants in the same state, which were cut off and weighed immediately. Placed on filter paper at room temperature for 0 h, 1 h, 2 h, 3 h, 4 h, 5 h, 6 h, 7 h, 8 h, and 9 h, and the leaves were weighed at each time point. Three biological replicates were performed for one experiment.

Protein purification

Recombinant proteins were expressed in *E. coli* transseta cells. For AsDOF25 protein purification, the protein expression was induced with 0.2 M IPTG, and the *E. coli* bacteria was cultured at 16 °C overnight. For AsHSFA2c protein purification, the protein expression was induced with 0.5 mM IPTG, and the *E. coli* bacteria was cultured at 28 °C overnight. Bacterial cells collected were resuspended in lysis buffer [1% Triton X-100, 50 mM Tris-HCl (pH 8.0), 200 mM NaCl, 1 mM DTT, and 1 pellet per 50 mL of complete EDTA-free protease inhibitor (Roche)] and lysis by sonication. After centrifugation, supernatants were affinity-extracted with Glutathione Sepharose 4B[138].

Electrophoretic mobility shift assay

Purified GST-AsDOF25 protein or GST-AsHSFA2c protein were incubated with biotinylated or non-biotinylated double-stranded DNA in the binding

buffer (Thermo) at room temperature for 25 min. The binding reaction mixture was resolved with 6% native PAGE at 4 °C. The interaction between proteins and DNA probes was detected by LightShift™ EMSA Optimization and Control Kit (Thermo)[139].

Leaf cell observation

The third leaf of trifoliate stage 'cv. Mengyan No.1' was treated with ethanol, which was soaked in 75% ethanol overnight. Then leaves were soaked in 2% methanol containing 0.24 M HCl for 25 min at 37 °C. Followed, at room temperature, soaking in 60% ethanol containing and 7% NaOH for 25 min[139]. Leaves were observed with a stereoscope.

Protein extraction and western blot

Total protein was extracted by the extraction buffer [0.2 M NaCl, 5 mM $MgCl_2$, 5 mM DTT, 20 mM Tris-HCl (pH 7.5), 0.03% Tween-20 (Ameresco), and 0.5 tablets of protease inhibitor (Roche)]. The supernatant was collected by centrifuging at 12,000 rpm for 15 min. Total proteins were examined by western blot analysis using α-tubulin (1:5000; EASYBIO, BE0031) as a loading control. Proteins in the study were also probed with α-GFP (1:2000; EASYBIO, BE2001), α-H3 (1:2000; EASYBIO, BE7004), α-PEPC (1:2000; Agrisera, As09458). Secondary antibodies were goat anti-rabbit IgG (1:5000; EASYBIO, BE0101) and goat anti-mouse IgG (1:5000; EASYBIO, BE0102). The protein Marker (product #26616) purchased from Thermo Scientific was used in all the western blot assays in this manuscript. The instrument (BIO-01, O1900) was used to obtain images.

Protein colocalization in plants

To determine the subcellular localization of AsHSFA2c, *A. tumefaciens* containing *pAsHSFA2c::AsHSFA2c-GFP* was inoculated in *N. benthamiana*, respectively. The images were taken under confocal fluorescence microscopy (LSM900).

Isolation and purification of nucleus and cytoplasm

3 g aerial parts of 4-week-old *N. benthamiana* under 12-h light/12-h dark photoperiod were ground to a fine powder in liquid nitrogen and were homogenized with 10 mL nuclei isolation buffer (20 mM Tris-HCl (pH 7.4), 5 mM $MgCl_2$, 25% glycerol, and 5 mM DTT) at 4 °C. The homogenate was filtered through a double layer of Miracloth, and the resulting flow-through was centrifuged at 200 g for 5 min at 4 °C. The supernatant consisting of the cytoplasmic fraction was collected by 12,000 g centrifugation for 10 min at 4 °C and the pellet was washed five times with nuclear wash buffer (20 mM Tris-HCl (pH 7.4), 5 mM $MgCl_2$, 25% glycerol, 5 mM DTT, and 0.2% Triton X-100) at 1500 g for 3 min. α-H3 (1:2000; EASYBIO, BE7004) and α-PEPC (1:2000; Agrisera, As09458) were used as nuclear and cytoplasmic protein marker, respectively[140].

Nuclear run-on assay

To determine the transcription after drought treatment, 3 g trifoliate stage oat leaves were collected. Briefly, plant samples were ground in liquid nitrogen and were suspended in 30 mL lysis buffer (20 mM Tris-HCl (pH 7.5), 20 mM KCl, 2 mM EDTA (pH 8.0), 2.5 mM $MgCl_2$, 25% Glycerol, 250 mM Sucrose, 5 mM DTT, 1 pellet per 50 mL of cOmplete EDTA-free protease inhibitor)[139,140]. After centrifugation at 4 °C, the precipitate was washed four times with NRBT buffer (20 mM Tris-HCl (pH 7.4), 25% Glycerol, 2.5 mM $MgCl_2$, 0.2% Triton X-100, 4 mM DTT). Then, precipitates were resuspended with nuclei storage buffer (50 mM Tris-HCl (pH 7.8), 1 mM DTT, 20% Glycerol, 5 mM $MgCl_2$, 0.44 M Sucrose) and added to the transcription system:10 μL 10× Transcription buffer (50 mM Tris-HCl (pH 7.5), 5 mM $MgCl_2$, 150 mM KCl, 0.2% Sarkosyl, 20 U/mL RNase inhibitor, 1 mM DTT), 5 μL NTP mixture (100 mM ATP, 100 mM CTP, 100 mM GTP, 100 mM BrUTP) and 35 μL RNase-free H_2O. The run-on reaction was performed at 37 °C for 45 min. Total RNA was extracted from the transcription system using TRIzol reagent followed by DNase I (NEB) treatment. The purified RNAs were incubated with 60 μL anti-BrdU beads (Santa Cruz) at 4 °C for 2 h. After IP, beads were washed twice with low-salt buffer (0.2 × SSPE (0.03 M NaCl, 2 mM NaH_2PO_4, 0.2 mM EDTA, pH 7.4), 1 mM EDTA (pH 8.0), 0.05% Tween-20) and then twice with high-salt buffer (0.5 × SSPE (0.075 M NaCl, 5 mM NaH_2PO_4, 0.5 mM EDTA, pH 7.4), 0.05% Tween-20, 37.5 mM NaCl, 1 mM EDTA (pH 8.0)) at 4 °C. The precipitated RNA was extracted using TRIzol reagent and used for qRT-PCR analysis.

Chlorophyll measurement

The leaves were incubated in 95% (*v*/*v*) ethanol for 5 days in darkness to obtain a solution containing chlorophyll. The absorbances were measured at 665 and 649 nm. The chlorophyll contents were calculated according to the following ratio: $(6.63A_{665} + 18.08A_{649})$/g fresh weight[141].

Statistics and reproducibility

The analysis was performed using GraphPad Prism version 6.01 (San Diego, California, USA). Sample sizes were chosen based on previous publications[12,13,111,142–144], the detailed specifics are presented in the corresponding methods section. Each value shown for each group is the mean ± SD (standard deviation). The *p* value was calculated using Student's *t*-test (two-tailed). p values < 0.05 were considered significant, while p values > 0.05 were considered non-significant. Each images represent at least three independent biological repeats.

Reporting summary

Further information on research design is available in the Nature Portfolio Reporting Summary linked to this article.

Data availability

High-throughput sequencing data obtained in this study has been submitted to the Genome Sequence Archive (GSA) database (https://ngdc.cncb.ac.cn/gsa/) at the National Genomics Data Center (NGDC), with BioProject accession number PRJCA024610. The numeral source data for graphs and charts of the main figure in the manuscript are provided in Supplementary Data 19. Uncropped images of the figures are included in Supplementary Information (Supplemental Fig. 20–30). The authors declare that all other data are available in the article and its Supplementary Information Files or from the corresponding author on reasonable request.

Code availability

In this study, all software utilized was open-access, with parameters clearly outlined in the Methods section. When specific software parameters were not detailed, the default settings recommended by the developers were applied.

Received: 15 July 2024; Accepted: 28 February 2025;
Published online: 08 March 2025

References

1. Gong, Z. et al. Plant abiotic stress response and nutrient use efficiency. *Sci. China Life Sci.* **63**, 635–674 (2020).
2. Gupta, A., Rico-Medina, A. & Caño-Delgado, A. I. The physiology of plant responses to drought. *Science* **368**, 266–269 (2020).
3. Mao, H. et al. Variation in cis-regulation of a NAC transcription factor contributes to drought tolerance in wheat. *Mol. Plant* **15**, 276–292 (2022).
4. Zhang, H., Zhu, J., Gong, Z. & Zhu, J.-K. Abiotic stress responses in plants. *Nat. Rev. Genet.* **23**, 104–119 (2022).
5. González, E. M. Drought stress tolerance in plants. *Int. J. Mol. Sci.* **24**, 6562 (2023).
6. Kamal, N. et al. The mosaic oat genome gives insights into a uniquely healthy cereal crop. *Nature* **606**, 113–119 (2022).
7. Peng, Y. et al. Reference genome assemblies reveal the origin and evolution of allohexaploid oat. *Nat. Genet.* **54**, 1248–1258 (2022).
8. Rasane, P., Jha, A., Sabikhi, L., Kumar, A. & Unnikrishnan, V. S. Nutritional advantages of oats and opportunities for its processing

as value added foods—a review. *J. Food Sci. Technol.* **52**, 662–675 (2015).
9. Zhang, H., Zhao, Y. & Zhu, J.-K. Thriving under stress: how plants balance growth and the stress response. *Dev. Cell* **55**, 529–543 (2020).
10. Du, P. et al. WRKY transcription factors and OBERON histone-binding proteins form complexes to balance plant growth and stress tolerance. *EMBO J.* **42**, e113639 (2023).
11. Lv, A. et al. The MsDHN1-MsPIP2;1-MsmMYB module orchestrates the trade-off between growth and survival of alfalfa in response to drought stress. *Plant Biotechnol. J.* **22**, 1132–1145 (2024).
12. Xie, Z. et al. OsNAC120 balances plant growth and drought tolerance by integrating GA and ABA signaling in rice. *Plant Commun.* **5**, 100782 (2024).
13. Yin, C. et al. The dynamics of H2A.Z on SMALL AUXIN UP RNAs regulate abscisic acid-auxin signaling crosstalk in Arabidopsis. *J. Exp. Bot.* **74**, 4158–4168 (2023).
14. Li, X.-T., Feng, X.-Y., Zeng, Z., Liu, Y. & Shao, Z.-Q. Comparative analysis of HSF genes from secale cereale and its triticeae relatives reveal ancient and recent gene expansions. *Front. Genet.* **12**, 801218 (2021).
15. Bechtold, U. et al. Arabidopsis HEAT SHOCK TRANSCRIPTION FACTORA1b overexpression enhances water productivity, resistance to drought, and infection. *J. Exp. Bot.* **64**, 3467–3481 (2013).
16. Tan, B. et al. Genome-wide identification of HSF family in peach and functional analysis of *PpHSF5* involvement in root and aerial organ development. *PeerJ* **9**, e10961 (2021).
17. Ren, Y. et al. Genome-wide identification, phylogenetic and expression pattern analysis of HSF family genes in the Rye (Secale cereale L.). *BMC Plant Biol.* **23**, 441 (2023).
18. Liu, A.-L. et al. Over-expression of *OsHsfA7* enhanced salt and drought tolerance in transgenic rice. *BMB Rep.* **46**, 31–36 (2013).
19. Xiang, J. et al. Heat shock factor OsHsfB2b negatively regulates drought and salt tolerance in rice. *Plant Cell Rep.* **32**, 1795–1806 (2013).
20. Li, P.-S. et al. Genome-wide analysis of the Hsf family in soybean and functional identification of *GmHsf-34* involvement in drought and heat stresses. *BMC Genomics* **15**, 1009 (2014).
21. Wang, J. et al. A novel heat shock transcription factor (ZmHsf08) negatively regulates salt and drought stress responses in maize. *Int. J. Mol. Sci.* **22**, 11922 (2021).
22. Bi, H. et al. Characterization of the wheat heat shock factor TaHsfA2e-5D conferring heat and drought tolerance in arabidopsis. *Int. J. Mol. Sci.* **23**, 2784 (2022).
23. Jin, X. F. et al. OsAREB1, an ABRE-binding protein responding to ABA and glucose, has multiple functions in Arabidopsis. *BMB Rep.* **43**, 34–39 (2010).
24. Miao, J. et al. OsPP2C09, a negative regulatory factor in abscisic acid signalling, plays an essential role in balancing plant growth and drought tolerance in rice. *N. Phytol.* **227**, 1417–1433 (2020).
25. Zhang, S.-W. et al. Altered architecture and enhanced drought tolerance in rice via the down-regulation of indole-3-acetic acid by TLD1/OsGH3.13 activation. *Plant Physiol.* **151**, 1889–1901 (2009).
26. Ma, W.-T. & Fan, W.-G. [Relationship between drought resistance and endogenous hormone content in different citrus species. *Ying Yong Sheng Tai Xue Bao* **25**, 147–154 (2014).
27. Chen, M. et al. Knockout of auxin response factor SlARF4 improves tomato resistance to water deficit. *Int. J. Mol. Sci.* **22**, 3347 (2021).
28. Verma, S., Negi, N. P., Pareek, S., Mudgal, G. & Kumar, D. Auxin response factors in plant adaptation to drought and salinity stress. *Physiol. Plant* **174**, e13714 (2022).
29. Liu, J., Carriquí, M., Xiong, D. & Kang, S. Influence of IAA and ABA on maize stem vessel diameter and stress resistance in variable environments. *Physiol. Plant* **176**, e14443 (2024).
30. Bind, M. A. C. & Rubin, D. B. When possible, report a Fisher-exact P value and display its underlying null randomization distribution. *Proc. Natl. Acad. Sci. USA* **117**, 19151–19158 (2020).
31. Butts, J. C. et al. A single-cell transcriptomic map of the developing Atoh1 lineage identifies neural fate decisions and neuronal diversity in the hindbrain. *Dev Cell* **59**, 2171–2188 (2024).
32. Wang, C. et al. Exogenous spraying of IAA improved the efficiency of microspore embryogenesis in Wucai (Brassica campestris L.) by affecting the balance of endogenous hormones, energy metabolism, and cell wall degradation. *BMC Genomics* **24**, 380 (2023).
33. Li, T. et al. Autocatalytic biosynthesis of abscisic acid and its synergistic action with auxin to regulate strawberry fruit ripening. *Hortic Res* **9**, uhab076 (2022).
34. Cutler, S. R., Rodriguez, P. L., Finkelstein, R. R. & Abrams, S. R. Abscisic acid: emergence of a core signaling network. *Annu Rev. Plant Biol.* **61**, 651–679 (2010).
35. Fidler, J. et al. PYR/PYL/RCAR receptors play a vital role in the abscisic-acid-dependent responses of plants to external or internal stimuli. *Cells* **11**, 517–527 (2022).
36. Wang, H., Liu, S., Fan, F., Yu, Q. & Zhang, P. A Moss 2-oxoglutarate/Fe(II)-dependent dioxygenases (2-ODD) gene of flavonoids biosynthesis positively regulates plants abiotic stress tolerance. *Front. Plant Sci.* **13**, 850062 (2022).
37. You, Z. et al. The CBL1/9-CIPK1 calcium sensor negatively regulates drought stress by phosphorylating the PYLs ABA receptor. *Nat. Commun.* **14**, 5886 (2023).
38. Liu, C., Wu, Y. & Wang, X. bZIP transcription factor OsbZIP52/RISBZ5: a potential negative regulator of cold and drought stress response in rice. *Planta* **235**, 1157–1169 (2012).
39. Raineri, J., Wang, S., Peleg, Z., Blumwald, E. & Chan, R. L. The rice transcription factor OsWRKY47 is a positive regulator of the response to water deficit stress. *Plant Mol. Biol.* **88**, 401–413 (2015).
40. Shim, J. S. et al. Overexpression of OsNAC14 improves drought tolerance in rice. *Front Plant Sci.* **9**, 310 (2018).
41. Yan, L. et al. A novel SAPK10-WRKY87-ABF1 biological pathway synergistically enhance abiotic stress tolerance in transgenic rice (*Oryza sativa*). *Plant Physiol. Biochem.* **168**, 252–262 (2021).
42. Wang, H. et al. Dehydration-responsive element binding protein 1C, 1E, and 1G promote stress tolerance to chilling, heat, drought, and salt in rice. *Front. Plant Sci.* **13**, 851731 (2022).
43. Huang, D., Wu, W., Abrams, S. R. & Cutler, A. J. The relationship of drought-related gene expression in *Arabidopsis thaliana* to hormonal and environmental factors. *J. Exp. Bot.* **59**, 2991–3007 (2008).
44. Guo, D. & Qin, G. EXB1/WRKY71 transcription factor regulates both shoot branching and responses to abiotic stresses. *Plant Signal Behav.* **11**, e1150404 (2016).
45. Liu, Z. et al. Phytocytokine signalling reopens stomata in plant immunity and water loss. *Nature* **605**, 332–339 (2022).
46. Rachowka, J., Anielska-Mazur, A., Bucholc, M., Stephenson, K. & Kulik, A. SnRK2.10 kinase differentially modulates expression of hub WRKY transcription factors genes under salinity and oxidative stress in Arabidopsis thaliana. *Front. Plant Sci.* **14**, 1135240 (2023).
47. Zhang, P. et al. The long non-coding RNA DANA2 positively regulates drought tolerance by recruiting ERF84 to promote JMJ29-mediated histone demethylation. *Mol. Plant* **16**, 1339–1353 (2023).
48. Abe, H. et al. Arabidopsis AtMYC2 (bHLH) and AtMYB2 (MYB) function as transcriptional activators in abscisic acid signaling. *Plant Cell* **15**, 63–78 (2003).
49. Xu, B.-Q. et al. SlMYC2 mediates stomatal movement in response to drought stress by repressing SlCHS1 expression. *Front. Plant Sci.* **13**, 952758 (2022).
50. Lee, B.-R. et al. Differential response of phenylpropanoid pathway as linked to hormonal change in two Brassica napus cultivars contrasting drought tolerance. *Physiol. Plant* **175**, e14115 (2023).

51. Shamloo-Dashtpagerdi, R., Shahriari, A. G., Tahmasebi, A. & Vetukuri, R. R. Potential role of the regulatory miR1119-MYC2 module in wheat (*Triticum aestivum* L.) drought tolerance. *Front Plant Sci.* **14**, 1161245 (2023).
52. Deng, Y. & He, Z. The seesaw action: balancing plant immunity and growth. *Sci. Bull. (Beijing)* **69**, 3–6 (2024).
53. Zhao, X.-L., Shi, Z.-Y., Peng, L.-T., Shen, G.-Z. & Zhang, J.-L. An atypical HLH protein OsLF in rice regulates flowering time and interacts with OsPIL13 and OsPIL15. *N. Biotechnol.* **28**, 788–797 (2011).
54. Todaka, D. et al. Rice phytochrome-interacting factor-like protein OsPIL1 functions as a key regulator of internode elongation and induces a morphological response to drought stress. *Proc. Natl. Acad. Sci. USA* **109**, 15947–15952 (2012).
55. Wang, Q. et al. OsDOG1L-3 regulates seed dormancy through the abscisic acid pathway in rice. *Plant Sci.* **298**, 110570 (2020).
56. Zhang, N. et al. A core regulatory pathway controlling rice tiller angle mediated by the LAZY1-dependent asymmetric distribution of auxin. *Plant Cell* **30**, 1461–1475 (2018).
57. Hu, Y. et al. *OsHOX1* and *OsHOX28* redundantly shape rice tiller angle by reducing *HSFA2D* expression and auxin content. *Plant Physiol.* **184**, 1424–1437 (2020).
58. Zhang, Y. et al. *OsHsfB4b* confers enhanced drought tolerance in transgenic arabidopsis and rice. *Int. J. Mol. Sci.* **23**, 10830 (2022).
59. Chen, X. et al. Maize transcription factor Zmdof1 involves in the regulation of *Zm401* gene. *Plant Growth Regul*. **66**, 271–284 (2012).
60. Gupta, S., Arya, G. C., Malviya, N., Bisht, N. C. & Yadav, D. Molecular cloning and expression profiling of multiple Dof genes of Sorghum bicolor (L) Moench. *Mol. Biol. Rep.* **43**, 767–774 (2016).
61. Sun, S. et al. Genome-wide analysis of *BpDof* genes and the tolerance to drought stress in birch (Betula platyphylla). *PeerJ* **9**, e11938 (2021).
62. Rasool, F. et al. Transcriptome unveiled the gene expression patterns of root architecture in drought-tolerant and sensitive wheat genotypes. *Plant Physiol. Biochem.* **178**, 20–30 (2022).
63. Li, W. et al. Transcriptional regulation of arabidopsis MIR168a and argonaute1 homeostasis in abscisic acid and abiotic stress responses. *Plant Physiol.* **158**, 1279–1292 (2012).
64. Westwood, J. H. et al. A viral RNA silencing suppressor interferes with abscisic acid-mediated signalling and induces drought tolerance in Arabidopsis thaliana. *Mol. Plant Pathol.* **14**, 158–170 (2013).
65. Du, F. et al. Dose-dependent AGO1-mediated inhibition of the miRNA165/166 pathway modulates stem cell maintenance in arabidopsis shoot apical meristem. *Plant Commun.* **1**, 100002 (2020).
66. Xu, C., Fang, X., Lu, T. & Dean, C. Antagonistic cotranscriptional regulation through ARGONAUTE1 and the THO/TREX complex orchestrates FLC transcriptional output. *Proc. Natl. Acad. Sci. USA* **118**, e2113757118 (2021).
67. Khan, M. I. R. et al. Improving drought tolerance in rice: Ensuring food security through multi-dimensional approaches. *Physiol. Plant* **172**, 645–668 (2021).
68. Hagen G. Auxin signal transduction. *Essays Biochem.* **58**, 1–12 (2015).
69. Verma, V., Ravindran, P. & Kumar, P. P. Plant hormone-mediated regulation of stress responses. *BMC Plant Biol.* **16**, 86 (2016).
70. Ma, H. et al. MAPK kinase 10.2 promotes disease resistance and drought tolerance by activating different MAPKs in rice. *Plant J.* **92**, 557–570 (2017).
71. Chen, P. et al. The apple DNA-binding one zinc-finger protein MdDof54 promotes drought resistance. *Hortic. Res.* **7**, 195 (2020).
72. Tan, M., et al. Polyamines metabolism interacts with γ-aminobutyric acid, proline and nitrogen metabolisms to affect drought tolerance of creeping bentgrass. *Int. J. Mol. Sci.* **23**, 2779 (2022).
73. Zhang, J. et al. Hsf and Hsp gene families in Populus: genome-wide identification, organization and correlated expression during development and in stress responses. *BMC Genomics* **16**, 181 (2015).
74. Dossa, K., Diouf, D. & Cissé, N. Genome-wide investigation of Hsf genes in sesame reveals their segmental duplication expansion and their active role in drought stress response. *Front. Plant Sci.* **7**, 1522 (2016).
75. He, F.-J., Zhu, F., Lu, M.-X. & Du, Y.-Z. Comparison of morphology, development and expression patterns of hsf and hsp11.0 of Cotesia chilonis under normal and high temperature. *PeerJ* **9**, e11353 (2021).
76. Iqbal, M. Z. et al. A heat shock transcription factor TrHSFB2a of white clover negatively regulates drought, heat and salt stress tolerance in transgenic arabidopsis. *Int. J. Mol. Sci.* **23**, 12769 (2022).
77. Wang, Q. et al. Hsf transcription factor gene family in peanut (*Arachis hypogaea* L.): genome-wide characterization and expression analysis under drought and salt stresses. *Front Plant Sci.* **14**, 1214732 (2023).
78. Yu, L. et al. Regulation of a single inositol 1-phosphate synthase homeologue by HSFA6B contributes to fibre yield maintenance under drought conditions in upland cotton. *Plant Biotechnol. J.* **22**, 2756–2772 (2024).
79. Sato, Y. et al. RiceXPro: a platform for monitoring gene expression in japonica rice grown under natural field conditions. *Nucleic Acids Res.* **39**, D1141–D1148 (2011).
80. Iwakawa, H.-O. & Tomari, Y. Life of RISC: formation, action, and degradation of RNA-induced silencing complex. *Mol. Cell* **82**, 30–43 (2022).
81. Ramasamy, M. et al. A sugarcane G-protein-coupled receptor, ShGPCR1, confers tolerance to multiple abiotic stresses. *Front. Plant Sci.* **12**, 745891 (2021).
82. Zhao, M. et al. The osmotic stress-activated receptor-like kinase DPY1 mediates SnRK2 kinase activation and drought tolerance in Setaria. *Plant Cell* **35**, 3782–3808 (2023).
83. Toriyama, T. et al. Sensor histidine kinases mediate ABA and osmostress signaling in the moss Physcomitrium patens. *Curr. Biol.* **32**, 164–175 (2022).
84. Hsu, P.-K., Dubeaux, G., Takahashi, Y. & Schroeder, J. I. Signaling mechanisms in abscisic acid-mediated stomatal closure. *Plant J.* **105**, 307–321 (2021).
85. Zhao, X., Xu, M., Wei, R. & Liu, Y. Expression of OsCAS (calcium-sensing receptor) in an arabidopsis mutant increases drought tolerance. *PLoS One* **10**, e0131272 (2015).
86. Huang, G.-T. et al. Signal transduction during cold, salt, and drought stresses in plants. *Mol. Biol. Rep.* **39**, 969–987 (2012).
87. de Zelicourt, A., Colcombet, J. & Hirt, H. The role of MAPK modules and ABA during abiotic stress signaling. *Trends Plant Sci.* **21**, 677–685 (2016).
88. Zhu, J.-K. Abiotic stress signaling and responses in plants. *Cell* **167**, 313–324 (2016).
89. Chen, X. et al. Protein kinases in plant responses to drought, salt, and cold stress. *J. Integr. Plant Biol.* **63**, 53–78 (2021).
90. Liu, H. et al. Signaling transduction of ABA, ROS, and Ca2+ in plant stomatal closure in response to drought. *Int. J. Mol. Sci.* **23**, 14824 (2022).
91. Rymen, B. et al. ABA suppresses root hair growth via the OBP4 transcriptional regulator. *Plant Physiol.* **173**, 1750–1762 (2017).
92. Wang, P., Yan, Z., Zong, X., Yan, Q. & Zhang, J. Genome-wide analysis and expression profiles of the dof family in cleistogenes songorica under temperature, salt and ABA treatment. *Plants* **10**, 850 (2021).
93. Zhai, Z. et al. Abscisic acid-responsive transcription factors PavDof2/6/15 mediate fruit softening in sweet cherry. *Plant Physiol.* **190**, 2501–2518 (2022).
94. Li, Y. et al. GhDof1.7, a Dof transcription factor, plays positive regulatory role under salinity stress in upland cotton. *Plants* **12**, 3740 (2023).

95. Singh, D. & Laxmi, A. Transcriptional regulation of drought response: a tortuous network of transcriptional factors. *Front. Plant Sci.* **6**, 895 (2015).
96. Alabd, A. et al. ABRE-BINDING FACTOR3-WRKY DNA-BINDING PROTEIN44 module promotes salinity-induced malate accumulation in pear. *Plant Physiol.* **192**, 1982–1996 (2023).
97. Geng, L. et al. Transcription factor RcNAC091 enhances rose drought tolerance through the abscisic acid-dependent pathway. *Plant Physiol.* **193**, 1695–1712 (2023).
98. Skirycz, A. et al. DOF transcription factor AtDof1.1 (OBP2) is part of a regulatory network controlling glucosinolate biosynthesis in Arabidopsis. *Plant J.* **47**, 10–24 (2006).
99. Carranco, R., Espinosa, J. M., Prieto-Dapena, P., Almoguera, C. & Jordano, J. Repression by an auxin/indole acetic acid protein connects auxin signaling with heat shock factor-mediated seed longevity. *Proc. Natl. Acad. Sci. USA* **107**, 21908–21913 (2010).
100. Xu, Z. et al. New insight into the molecular basis of cadmium stress responses of wild paper mulberry plant by transcriptome analysis. *Ecotoxicol. Environ. Saf.* **171**, 301–312 (2019).
101. Sajjad, M., Wei, X., Liu, L., Li, F. & Ge, X. Transcriptome analysis revealed GhWOX4 intercedes myriad regulatory pathways to modulate drought tolerance and vascular growth in cotton. *Int. J. Mol. Sci.* **22**, 898 (2021).
102. Zhu, M.-D. et al. Rice *OsHSFA3* gene improves drought tolerance by modulating polyamine biosynthesis depending on abscisic acid and ROS levels. *Int. J. Mol. Sci.* **21**, 1857 (2020).
103. Wei, J.-T. et al. GmDof41 regulated by the DREB1-type protein improves drought and salt tolerance by regulating the DREB2-type protein in soybean. *Int J. Biol. Macromol.* **230**, 123255 (2023).
104. Ma, Z. et al. Upregulation of wheat heat shock transcription factor TaHsfC3-4 by ABA contributes to drought tolerance. *Int. J. Mol. Sci.* **25**, 977 (2024).
105. Jan, A., Kitano, H., Matsumoto, H. & Komatsu, S. The rice OsGAE1 is a novel gibberellin-regulated gene and involved in rice growth. *Plant Mol. Biol.* **62**, 439–452 (2006).
106. Hong, Y., Yuan, S., Sun, L., Wang, X. & Hong, Y. Cytidinediphosphate-diacylglycerol synthase 5 is required for phospholipid homeostasis and is negatively involved in hyperosmotic stress tolerance. *Plant J.* **94**, 1038–1050 (2018).
107. Gonzalez, N., Vanhaeren, H. & Inzé, D. Leaf size control: complex coordination of cell division and expansion. *Trends Plant Sci.* **17**, 332–340 (2012).
108. de Lucas, M. & Prat, S. PIFs get BRright: PHYTOCHROME INTERACTING FACTORs as integrators of light and hormonal signals. *N. Phytol.* **202**, 1126–1141 (2014).
109. Iqbal, N. et al. Ethylene role in plant growth, development and senescence: interaction with other phytohormones. *Front. Plant Sci.* **8**, 475 (2017).
110. Liu, X. & Hou, X. Antagonistic regulation of ABA and GA in metabolism and signaling pathways. *Front. Plant Sci.* **9**, 251 (2018).
111. Liu, D. et al. Comparative transcriptome profiling reveals the multiple levels of crosstalk in phytohormone networks in Brassica napus. *Plant Biotechnol. J.* **21**, 1611–1627 (2023).
112. Salehin, M. et al. Auxin-sensitive Aux/IAA proteins mediate drought tolerance in Arabidopsis by regulating glucosinolate levels. *Nat. Commun.* **10**, 4021 (2019).
113. Gao, J. et al. RRS1 shapes robust root system to enhance drought resistance in rice. *N. Phytol.* **238**, 1146–1162 (2023).
114. Su, P. et al. The Aux/IAA protein TaIAA15-1A confers drought tolerance in Brachypodium by regulating abscisic acid signal pathway. *Plant Cell Rep.* **42**, 385–394 (2023).
115. Iqbal, M. Z. et al. Overexpression of auxin/indole-3-acetic acid gene TrIAA27 enhances biomass, drought, and salt tolerance in *Arabidopsis thaliana*. *Plants* **13**, (2024).
116. Zhang, Y., Li, Y., Hassan, M. J., Li, Z. & Peng, Y. Indole-3-acetic acid improves drought tolerance of white clover via activating auxin, abscisic acid and jasmonic acid related genes and inhibiting senescence genes. *BMC Plant Biol.* **20**, 150 (2020).
117. Kim, D., Langmead, B. & Salzberg, S. L. HISAT: a fast spliced aligner with low memory requirements. *Nat. Methods* **12**, 357–360 (2015).
118. Kovaka, S. et al. Transcriptome assembly from long-read RNA-seq alignments with StringTie2. *Genome Biol.* **20**, 278 (2019).
119. Han, L. et al. A multi-omics integrative network map of maize. *Nat. Genet* **55**, 144–153 (2023).
120. Li, D. et al. Integrative multi-omics analysis reveals genetic and heterotic contributions to male fertility and yield in potato. *Nat. Commun.* **15**, 8652 (2024).
121. Li, F., Hu, Q., Chen, F. & Jiang, J. F. Transcriptome analysis reveals Vernalization is independent of cold acclimation in Arabidopsis. *BMC Genomics* **22**, 462 (2021).
122. Zhang, S.-Q. et al. Combined effect of microplastic and triphenyltin: Insights from the gut-brain axis. *Environ. Sci. Ecotechnol.* **16**, 100266 (2023).
123. Minh, B. Q. et al. IQ-TREE 2: new models and efficient methods for phylogenetic inference in the genomic era. *Mol. Biol. Evol.* **37**, 1530–1534 (2020).
124. Letunic, I. & Bork, P. Interactive tree of life (iTOL) v6: recent updates to the phylogenetic tree display and annotation tool. *Nucleic Acids Res.* **52**, W78–W82 (2024).
125. Bartlett, A. et al. Mapping genome-wide transcription-factor binding sites using DAP-seq. *Nat. Protoc.* **12**, 1659–1672 (2017).
126. Liu, Y. et al. MdERF114 enhances the resistance of apple roots to Fusarium solani by regulating the transcription of MdPRX63. *Plant Physiol.* **192**, 2015–2029 (2023).
127. Read, J. F. et al. Single cell transcriptomics reveals cell type specific features of developmentally regulated responses to lipopolysaccharide between birth and 5 years. *Front Immunol.* **14**, 1275937 (2023).
128. Sun, Y. et al. Single-cell transcriptomic analysis reveals the developmental trajectory and transcriptional regulatory networks of pigment glands in Gossypium bickii. *Mol. Plant* **16**, 694–708 (2023).
129. Yao, J. et al. Populus euphratica WRKY1 binds the promoter of H+-ATPase gene to enhance gene expression and salt tolerance. *J. Exp. Bot.* **71**, 1527–1539 (2020).
130. Zhang, Y. et al. Model-based analysis of ChIP-Seq (MACS). *Genome Biol.* **9**, R137 (2008).
131. Yuan, J. et al. GhRCD1 regulates cotton somatic embryogenesis by modulating the GhMYC3-GhMYB44-GhLBD18 transcriptional cascade. *N. Phytol.* **240**, 207–223 (2023).
132. Chen, C. et al. TBtools-II: a "one for all, all for one" bioinformatics platform for biological big-data mining. *Mol. Plant* **16**, 1733–1742 (2023).
133. Zhang, J. et al. Vacuum and co-cultivation agroinfiltration of (Germinated) seeds results in tobacco rattle virus (TRV) mediated whole-plant virus-induced gene silencing (VIGS) in wheat and maize. *Front. Plant Sci.* **8**, 393 (2017).
134. Wang, K. et al. The gene *TaWOX5* overcomes genotype dependency in wheat genetic transformation. *Nat. Plants* **8**, 110–117 (2022).
135. Ishida, Y., Tsunashima, M., Hiei, Y. & Komari, T. Wheat (*Triticum aestivum* L.) transformation using immature embryos. *Methods Mol. Biol.* **1223**, 189–198 (2015).
136. Liu, X. et al. Uncovering the transcriptional regulatory network involved in boosting wheat regeneration and transformation. *Nat. Plants* **9**, 908–925 (2023).
137. Yu, Y. et al. Enhancing wheat regeneration and genetic transformation through overexpression of TaLAX1. *Plant Commun.* **5**, 100738 (2024).
138. Li, Q. et al. DEAD-box helicases modulate dicing body formation in Arabidopsis. *Sci. Adv.* **7**, eabc6266 (2021).

139. Liu, N. et al. A lncRNA fine-tunes salicylic acid biosynthesis to balance plant immunity and growth. *Cell Host Microbe* **30**, 1124–1138 (2022).
140. Zhao, X. et al. Global identification of arabidopsis lncRNAs reveals the regulation of MAF4 by a natural antisense RNA. *Nat. Commun.* **9**, 5056 (2018).
141. Tian, T. et al. Arabidopsis FAR-RED ELONGATED HYPOCOTYL3 integrates age and light signals to negatively regulate leaf senescence. *Plant Cell* **32**, 1574–1588 (2020).
142. Jiang, Y. et al. Transcriptome analysis of drought-responsive and drought-tolerant mechanisms in maize leaves under drought stress. *Physiol. Plant* **175**, e13875 (2023).
143. Wang, G. et al. Functional analysis of a late embryogenesis abundant protein ZmNHL1 in maize under drought stress. *J. Plant Physiol.* **280**, 153883 (2023).
144. Tian, T. et al. Genome assembly and genetic dissection of a prominent drought-resistant maize germplasm. *Nat. Genet.* **55**, 496–506 (2023).

Acknowledgements

This work was supported by the Young Elite Scientists Sponsorship Program by CAST grant YESS20210080, the National Natural Science Foundation of China (32100500 and 32401776), the Natural Science Foundation of Hebei Province (grant no: C2021201048 and C2023201074) and the Interdisciplinary Research Program of Natural Science of Hebei University (grant no: 513201422004).

Author contributions

H.D. conceived and supervised the project. H.D. and N.L. designed the paper. N.L., W.L., Y.Q., and H.D. wrote the paper. Y.Q. sequenced and processed the raw data. N.L., W.L., Y.Q., C.D., Q.S., S.W., and Q.H. provided the methods. N.L. and Y.Q. screened candidate genes. N.L., Y.Y., and J.Y. made functional verification. N.L., Y.Q., and W.L. provided the original draft. H.D. and Z.G. funded the acquisition. All authors read and approved the final manuscript.

Competing interests

The authors declare no competing interests.

Additional information

Supplementary information The online version contains supplementary material available at https://doi.org/10.1038/s42003-025-07857-8.

Correspondence and requests for materials should be addressed to Huilong Du.

Peer review information *Communications Biology* thanks the anonymous reviewers for their contribution to the peer review of this work. Primary Handling Editors: Showkat Ganie and David Favero.